Realizations of vascularized tissues: from *in vitro* platforms to *in vivo* grafts

Bing Ren[1], Zhihua Jiang[2], Walter Lee Murfee[3], Adam J. Katz[4], Dietmar Siemann[5], Yong Huang[1,3,a]

[1]Department of Mechanical and Aerospace Engineering, University of Florida, Gainesville, FL 32611, USA

[2]Department of Surgery, University of Florida, Gainesville, FL 32610, USA

[3]Department of Biomedical Engineering, University of Florida, Gainesville, FL 32611, USA

[4]Department of Plastic and Reconstructive Surgery, Wake Forest School of Medicine, Winston-Salem, NC 27157, USA

[5]Department of Radiation Oncology, University of Florida, Gainesville, FL 32610, USA

[a]Author to whom correspondence should be addressed: yongh@ufl.edu.

Phone: 001-352-392-5520, Fax: 001- 352-392-7303

Abbreviations:
10T1/2s: C3H/10T1/2 cells
ADSCs: adipose-derived stem cells
CFs: cardiac fibroblasts
CMs: cardiomyocytes
DLP: digital light processing
ECM: extracellular matrix
FRESH: freeform reversible embedding of suspended hydrogels
GelMA: gelatin methacrylate
GMECs: glomerular microvascular endothelial cells
GM-HA: glycidal methacrylate-hyaluronic acid
GSCs: glioma stem cells
hADSCs: human adipose-derived stem cells
HBMECs: human brain microvascular endothelial cells
HCASMCs: human coronary artery smooth muscle cells
HDFs: human dermal fibroblasts
HDMVECs: human dermal microvascular endothelial cells
HepG2: hepatocellular carcinoma cells
hESC-ECs: embryonic stem cell-derived endothelial cells
hiPSC-ECs: human-induced pluripotent stem cell-derived endothelial cells
hiPSC-HPCs: human induced pluripotent stem cells derived hepatic progenitor cells
HLECs: human lung epithelial cells
HLFs: human lung fibroblasts
HLMVECs: human lung microvascular endothelial cells
HNDFs: human neonatal dermal fibroblast cells
hPSCs: human pluripotent stem cells
HUVECs: human umbilical vein endothelial cells
iPSCs: human induced pluripotent stem cells
iPSCs-CMs: induced pluripotent stem cells derived cardiomyocytes
iPSCs-ECs: induced pluripotent stem cells derived endothelial cells
MSCs: mesenchymal stem cells
NHDFs: normal human dermal fibroblasts
PDMS: polydimethylsiloxane
PEGDA: polypoly(ethylene glycol) diacrylate
POMaC: poly(octamethylene maleate (anhydride) citrate)
PTECs: proximal tubule epithelial cells
PVA: poly(vinyl alcohol)
RBCs: red blood cells
REC: renal epithelial cells
RPTEC: renal proximal tubular epithelial cells
SLA: stereolithography
SMCs: smooth muscle cells
SWIFT: sacrificial writing into functional tissue

Abstract:
Vascularization is essential for realizing thick and functional tissue constructs that can be

utilized for *in vitro* study platforms and *in vivo* grafts. The vasculature enables the transport of nutrients, oxygen, and wastes, and is also indispensable to organ functional units such as the nephron filtration unit, the blood-air barrier, and the blood-brain barrier. This review aims to discuss the latest progress of organ-like vascularized constructs with specific functionalities and realizations even though they are not yet ready to be used as organ substitutes. First, the human vascular system is briefly introduced and related design considerations for engineering vascularized tissues are discussed. Second, up-to-date creation technologies for vascularized tissues are summarized and classified into the engineering and cellular self-assembly approaches. Third, recent applications ranging from *in-vitro* tissue models, including generic vessel models, tumor models, and different human organ models such as heart, kidneys, liver, lungs, and brain, to prevascularized *in vivo* grafts for implantation and anastomosis are discussed in detail. The specific design considerations for the aforementioned applications are summarized and future perspectives regarding future clinical applications and commercialization are provided.

Keywords: biofabrication; vascularized tissue engineering; perfusable channels; vascular networks; endothelial cells

1. Introduction

Blood vessels, either large or capillary, are pivotal to transporting nutrients and oxygen to the tissues and organs as well as removing wastes and carbon dioxide. Due to diffusion limits, most living cells are located no more than 100-200 μm away from patent vessel networks; a factor of critical importance in engineering viable three-dimensional (3D) tissues or organs [1,2]. In addition to fulfilling the metabolic demands of tissues, blood vessels play an important role in various physiological niches, including nephron filtration units, the blood-air barrier in the lung, and the blood-brain barrier.

While the engineering of a whole regenerative organ is still in its infancy, the creation of vascularized tissues, either by an engineering approach and/or a biological self-assembly approach, has been of great interest in the biofabrication research community. Such vascularized tissues can be utilized for various biomedical applications, ranging from *in vitro* disease modeling and drug screening to *in vivo* implantation. For *in vitro* disease modeling and drug screening applications, vascularized tissues are more physiologically relevant due to their increasing tissue complexity and cellular fidelity, which provide biological insights that may not be readily available when using typical microfluidics-based organ-on-a-chip devices. For example, they can be used as models to study vascular disease progression [3] and the effect of hemodynamics on vasculopathy that may advance the development of therapeutics for various vascular diseases such as atherosclerosis, thrombosis, and stroke [4,5]. Besides blood vessel-related diseases, vascularized tissues can be employed in modeling physiological and/or pathological processes for organs and neoplasia [6-9]. Specific disease models also provide a versatile platform for high-throughput drug screening and new therapy development. Furthermore, studying basic organ biology, such as the effects of specific guidance cues, can be possible using an *in vitro* vascularized environment. For *in vivo* implantation applications, vascularized tissues may help facilitate immediate blood perfusion after anastomosis [10]. Generally, after the implantation of tissue-engineered grafts, a spontaneous network connecting with the host tissue develops, induced by the secretion of hypoxic signals and the inflammatory wound-healing response [11]. However, this ingrowth process is generally slow. It takes weeks for the *de novo* vascular network to penetrate a few millimeters, during which the interior cells run the risk of improper integration or even death [9,12]. This challenge

may be mitigated by creating engineered vascular networks in tissue grafts prior to implantation [13,14].

Despite the potential significance, engineering vascularized tissues remains a long-standing challenge that requires innovations in cell sources, extracellular biomaterials, chemical cues, fabrication methods, and more. To promote the development of vascularized tissues, this review summarizes the state-of-the-art realizations of 3D *in vitro* vascularized tissues made possible by using engineering and/or biological approaches. While relevant reviews focus on biomaterials [8,15,16] and biofabrication techniques [7,10,17-19], this review emphasizes the engineering of soft tissues with vessels and the ways these vascularized tissue models may be utilized as physiological and pathological research platforms, mimicking vessels, and tissues including heart, kidneys, liver, lungs, brain, and tumors. Purely perfusable models without living cell constituents are not discussed in this article and only tissue models which are not tissue-on-a-chip related are reviewed.

2. Human vascular system and design considerations

To be of relevance, the vascular system of an engineered vascularized tissue needs to recapitulate the physiological vascular characteristics and functionalities of in situ tissues [9,17]. Generally, human vessels are composed of different hierarchical levels: macrovessels (arteries and veins), which branch out into smaller vessels (arterioles and venules), and finally into capillaries [4,19,20] (Figure 1a). Large vessels, including arteries, veins, arterioles, and venules, have three layers: the inner layer (intima) of endothelial cells (ECs), the middle layer (media) of smooth muscle cells (SMCs) and elastic fibers, and the outer layer (adventitia) of connective tissues [16]. The EC layer lining the inner vessel wall acts as a barrier function for restricting the movement of blood cells and other circulating chemicals. SMCs are responsible for maintaining the vascular tone by constriction and relaxation in response to the pulsatile blood flow as well as local chemical and neurogenic regulations. The outmost connective tissue ensures good strength and durability. In contrast, capillaries only have a monolayer of ECs surrounded by a thin basal lamina and pericytes, where the exchange of oxygen and other chemicals occurs by either paracellular or transcellular transport. For mass delivery within engineered tissues, a dense capillary network with a functional EC interior layer is required to branch from the main vessels [17].

While ECs are indispensable, they may have different functions in different organs. For example, the endothelium of kidneys and liver has a fenestrated or discontinuous structure in response to the fast filtration requirements, while in the heart, lung, or brain, the endothelium barrier is tight and highly selective to restrict the exchange of certain molecules [17]. The functional difference of ECs is related to the difference in their tissue-specific phenotypes, which is known as the phenotypic heterogeneity [21]. Therefore, tissues with specific endothelium properties are needed to support diverse organ functions; the derivation of tissue-specific ECs from human pluripotent stem cells (hPSCs) may aid the creation of specialized tissue-specific models [22,23].

Natural human vessels form mainly by two processes: (i) vasculogenesis, which is the formation of new blood vessels during early embryonic development in the absence of pre-existing vessels, and (ii) angiogenesis, which is the sprouting of ECs and subsequential formation of new vessels from pre-existing vessels [11]. The vasculogenesis or angiogenesis potential helps grow neovessels and anastomose to a host tissue. However, the advance of spontaneous vessel sprouting is very low (<1 mm/day) [24], and this sprouting speed is not fast enough to support engineered tissues if they don't have pre-existing perfusable structures. Thus, an ideal engineered tissue should have perfusable structures and be able to integrate into the host tissue to enable instantaneous transportation of blood by direct surgical anastomosis [14].

In an engineered vascularized tissue, the primary role of the vascular system is to support the encapsulated cells through the delivery of nutrients and oxygen. Overall requirements of the engineered vasculature, including physical, anatomical, and functional requirements, are summarized in Table 1.

Table 1. Overall requirements of the engineered vasculature

Physical requirements	Anatomical and functional requirements
• Perfusable channels allowing blood/medium flow • Elasticity allowing constriction and relaxation in response to the pulsatile blood flow • Fatigue resistance under recurrent diastolic/systolic blood flow • Strength sustaining the burst pressure • Surgical suturing for *in vivo* implantation	• Multilayered structure mimicking real vessels • Vessel topology in a given tissue with regular or abnormal vascular segments as needed • Full functionality in terms of mass transport, filtration, and permeability

3. Creation technologies for vascularized tissues

While vascularized tissues can be created using various approaches such as co-culturing and seeding, complex 3D tissues (including thick ones) can be created using two different but complementary approaches: 1) an engineering approach to creating large diameter perfusable channels for EC seeding, usually for large-diameter vessels, and 2) a biological approach to self-assembling vascular and support cells into capillary structures, usually for small-diameter capillaries (Figure 1b). The engineering approach can be mainly implemented through casting and channel printing, including positive channel printing and negative channel printing. During casting, a template, such as a preformed object (such as a needle or nylon strand) [25-28], a molded template [29-31], and a 3D printed template [32-35], is utilized as a pattern in a chamber for subsequential hydrogel casting. Perfusable channels can be formed by removing the template after cross-linking the hydrogel matrix. Positive channel printing utilizes the direct creation of perfusable channels in a cross-linkable or cross-linked hydrogel matrix, and the pattern defines the channel(s) to be formed and is removed usually after the matrix is cross-linked. In this way, perfusable channels can be created by embedded sacrificial printing [36-39], photoablation [40], photodegradation [41], or sequential sacrificial printing [42-44]. Alternatively, negative channel printing refers to an approach during which a matrix is selectively cross-linked and solidified using a chemical or physical method while the rest matrix material undergoes no phase change and is subsequently removed, resulting in a channel structure as designed. Negative printing approaches include various light-assisted methods such as stereolithography (SLA) [45] and digital light processing (DLP) [46]. During SLA and DLP processes, the hydrogel matrix is selectively photo cross-linked layer by layer under photonic energy, and perfusable channels are formed after removing the uncross-linked hydrogel. Some key features of the aforementioned engineering approaches are summarized in Table 2.

While the engineering approaches facilitate the spatial arrangement of perfusable channel networks, creating capillaries of several microns remains challenging when using conventional engineering approaches due to the resolution limitation. Fortunately, due to the robust response of endothelial and perivascular cells to angiogenic stimulation, spontaneous neovascularization on the micrometer order can be induced by cellular self-assembly (Figure 1c) under the regulation of

various angiogenic biomolecular cues such as growth factors and extracellular matrix (ECM) proteins [4,47,48], resulting in the formation of vascular networks [49-51]. Human umbilical vein endothelial cells (HUVECs), human microvascular endothelial cells (HMVECs), and induced pluripotent stem cell-derived endothelial cells (iPSC-ECs) have primarily been employed as typical cell sources for endothelialization [15]. Since the promotion of angiogenesis can be attributed to cell-cell interactions and cellular secretions, incorporating multiple cell types in a co-culture environment offers an option to improve tissue fidelity in terms of structures, cell population, and functions, depending on the application scenarios. Technologies utilizing microfluidics [52,53], bioreactors [54,55], and co-culture [56] have been widely utilized to create microvessels with stimulated cellular self-assembly. Co-culture of the ECs with other support cells such as human lung fibroblasts (HLFs), normal human dermal fibroblasts (NHDFs) and human adipose-derived stem cells (hADSCs), mimicking the 3D complex tissue microenvironment, can stimulate the cell motility and facilitate the formation of microvessels [56-58]. As needed, the gradient of growth factors and shear stress can be utilized to guide the EC migration and capillary morphogenesis [4,39,48].

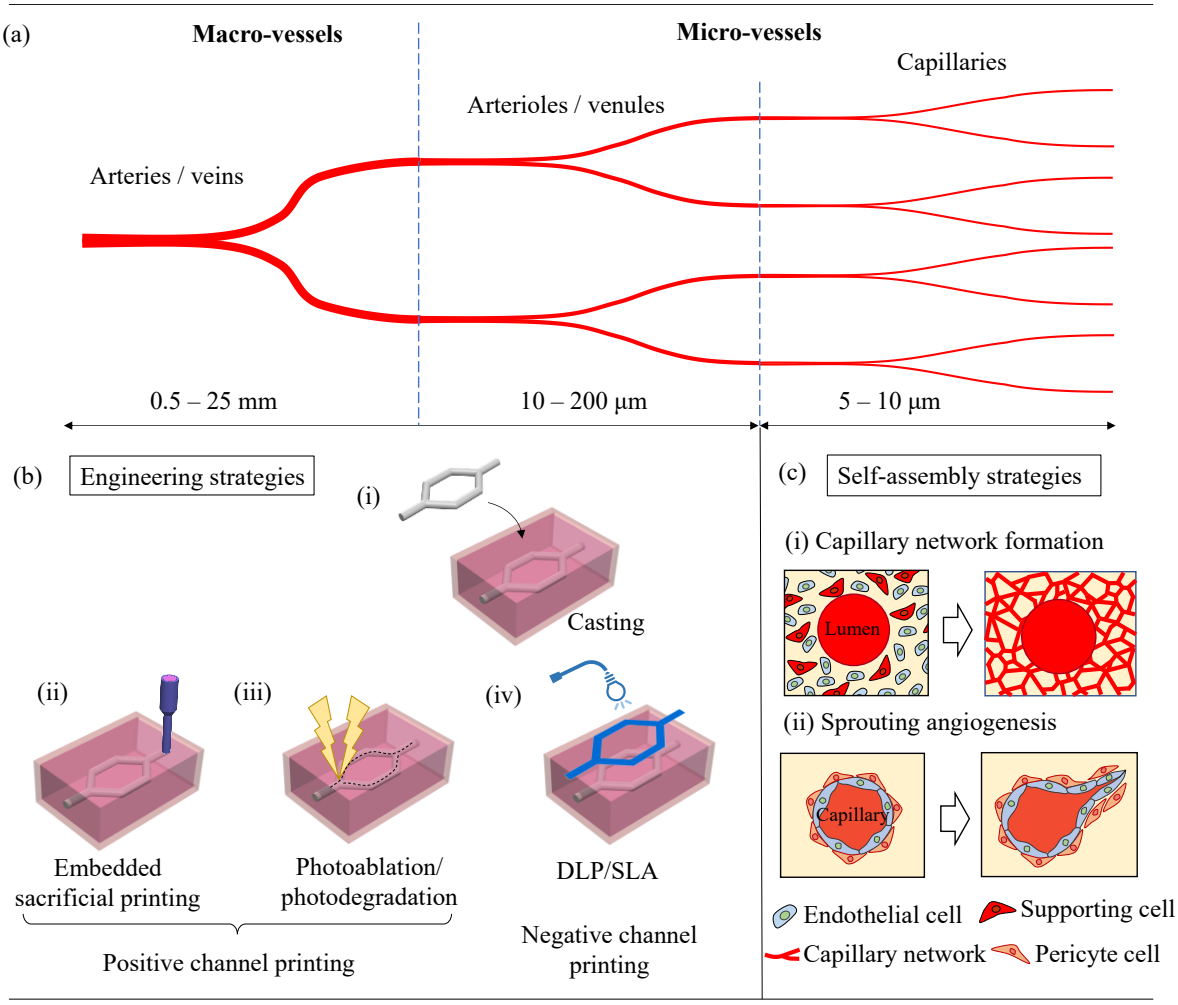

Figure 1. (a) Schematic of vascular system, and representation of current (b) engineering and (c) self-assembly strategies for vascularized tissue creation.

Table 2. Comparative summary of different engineering techniques for thick vascularized tissue fabrication.

Approach		Pros	Cons	Reference
Casting	By solid objects (stainless-steel needles/nylon wires)	Easily available	Limited structural complexity, usually used for straight channel fabrication	25-28
	By molded sacrificial templates	Improved structural complexity	Extra mold is required, lack of efficiency due to extra processes	29-31
	By 3D printed sacrificial templates	High design freedom, improved structural complexity	Good strength is required for printed templates	32-35
3D positive printing	Embedded printing	High design freedom, high structural complexity, achievable for multiple-layered channel fabrication	Support bath is required, limited printing resolution, interdiffusion between the bath and ink	36-39
	Photoablation/ photodegradation	High printing resolution	Cell injury concern	40, 41
	Sequential sacrificial printing	Good shape fidelity due to multiple gelling steps	Low efficiency, interface between different layers	42-44
3D negative printing	DLP/SLA	High printing resolution	Cell injury concern	45, 46

4. Realization of vascularized tissues

For this review, the realization of 1) high-fidelity *in vitro* vascularized tissue models for disease modeling or drug screening and 2) implantable *in vivo* artificial substitutes for damaged tissue regions are of particular interest. Each of these applications depends on biocompatible materials with appropriate strength and permeability, encapsulation of different living cells at varying concentrations, construction of 3D architectures with proper size and heterogeneity, and exposure to the physiologically relevant stimulus. For illustration purposes, generic vessel models, tumor models, and human organ-related models, including heart, kidneys, liver, lungs, and brain, are reviewed.

4.1. **Generic vessel models**

The vascular system plays an essential role in various processes in the human body, such as metabolic activities and homeostasis, which may be difficult to recapitulate and investigate *in vivo*. To address this issue, *in vitro* engineered vascularized tissues have been developed as vessel models to study the vascular biology science, vascular functions, hematological disease-related pathologies, and various cardiovascular diseases such as thrombosis, atherosclerosis, and stroke [3,59,60].

In terms of the vascular biology study, 3D endothelialized vessel models with perivascular cells encapsulated in the surrounding ECM allow the study of sprouting angiogenesis and endothelial-pericyte interactions [61] (Figure 2a). Mandrycky et al. [27] constructed a spiral microvessel model by molding it with a stainless steel spring in a collagen matrix (Figure 2b). Effects of the 3D curvature along with the flow conditions on the endothelial morphology and alignment were investigated. Understanding the phenotypic expression of ECs in response to the flow may guide the design of vascularization conditions for regenerative medicine applications.

In terms of disease models, Zhang et al. [32] fabricated a thrombosis-on-a-chip within a gelatin methacryloyl (GelMA) hydrogel matrix that consisted of microchannels lined with an EC monolayer (Figure 2c). Human whole blood that was induced to form thrombi by a $CaCl_2$ solution was infused into the channels in order to construct a biomimetic platform that could be used to study the pathologies of thrombosis, thrombolysis, and fibrosis. The endothelial barrier function is also of great research interest as one of the critical vascular functions. In some hematological and inflammatory diseases such as sickle-cell disease and malaria, endothelial-barrier dysfunction could occur due to inflammatory or infectious mediators. Qiu et al. [62] established a perfusable microvasculature-on-a-chip recapitulating the long-term endothelial barrier function for over one month. This enabled the study of endothelial barrier dysfunction and self-healing dynamics (Figure 2d). Straight or simple branched structures are typical designs for modeling basic vascular structures. Since irregular arterial geometries are useful for the recapitulation of turbulent blood flow-related diseases, Gao et al. [63] developed an *in vitro* atherosclerosis model with an improved relevance to these physiological conditions by involving the stenotic and curved features and further evaluated the therapeutic effects of atorvastatin (Figure 2e). Geometry-tunable vessel models may have the potential to serve as advanced platforms for investigating the hemodynamic forces, pathophysiology, and drug screening. By sensing the blood flow, which is categorized into laminar or turbulent, ECs respond differently in terms of the morphology and phenotype, thereby regulating the vascular formation.

In general, compared with conventional microfluidic vessel-on-a-chip models that use rigid polydimethylsiloxane (PDMS) for chip building, hydrogel material-based vascularized tissues provide a more physiologically relevant environment with a lower stiffness (hundreds of Pa to 50 kPa versus 50 kPa to several MPa of PDMS) and hence may hold greater potential as engineered vessel models [62,64]. When compared with *ex vivo* animal perfusion platforms such as the rat mesentery tissue containing real vascular networks [54], engineered vascularized tissues constructed using human cells may provide a better human-relevant environment for biomedical research.

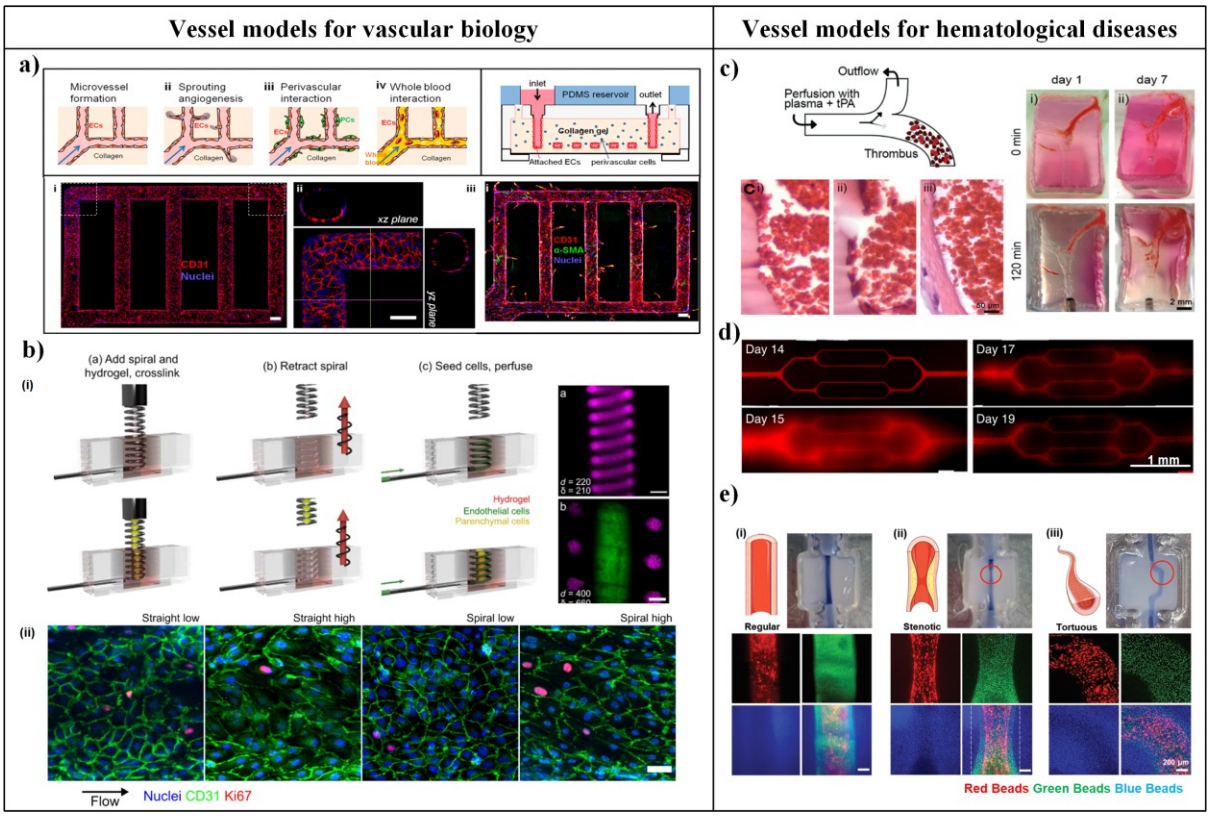

Figure 2. (a-b) Vessel models for vascular biology. a) fabrication of perfusable endothelialized channels within collagen gel and study of angiogenesis [61]. (Scale bars: 100 μm) b) Fabrication of 3D spiral vessel model for the study of endothelial response to flow conditions at curvature [27]. (i) Schematic of casting spiral channel structures by a stainless-steel spring in collagen hydrogels with (top) and without (bottom) a central lumen (scale bars: 500μm). (ii) Endothelial response to low and high flow conditions (Q = 1 and 50 μL/min) in straight and spiral vessels (scale bar: 50 μm). (c-e) Vessel models for hematological diseases. c) Thrombosis-on-a-chip with bifurcated enthothelialized microchannels and study of thrombosis/thrombolysis [32]. d) Vessel model for the study of endothelial barrier dysfunction and self-recovery [62]. e) Atherosclerotic model fabricated by embedded coaxial printing and achieved (i) regular straight, (ii) stenotic, and (iii) tortuous geometries [63].

4.2. **Tumor models**

The tumor microenvironment is highly complex consisting of diverse cellular composition (such as various host, neoplastic, and immune cells) and various physical and biochemical cues (such as those related to hypoxia and acidity). While challenging to develop, engineered 3D *in vitro* tumor models mimicking the complex tumor microenvironment (or tumor immune microenvironment) are highly sought after to serve as a platform for advanced cancer research [65]. As tumor vascularization is a critical process in tumor development, the incorporation of microvessels into tumor models aids the understanding of tumor-vessel dynamics [66]. The continuous support of nutrients and oxygen and the provision of tunable flow conditions should be considered in designing engineered tumor models for tumor activity studies and anticancer drug screening [67-70]. In addition, the morphology and function of tumor vessels are different from normal vessels. Tumor vessels are generally characterized by the unorganized capillary morphology, reduced blood flow, increased permeability, and local hypoxia [71]. More specifically, hallmarks of the unorganized morphology and associated altered function include loose pericyte wrapping along endothelial cells, enlarged capillary diameters, disrupted endothelial cell junctions, and endothelial gaps filled by immune or even cancer cells. The tumor vasculature can

be mechanistically linked to the increased expression of angiogenic factors that further contribute to increased vascular density. While it is challengeable to create a physiologically relevant vascularized tumor model, some promising results have been reported. Agarwal et al. [52] created a 3D vascularized tumor model for drug discovery, wherein avascular microtumors were obtained first as the building blocks and then assembled with ECs and other stromal cells 3D to realize the vascularization (Figure 3a). A 3D glioblastoma tumor model with perfusable vascular channels with which the cancer cell clusters were closely associated, can be used to model glioma/vascular cell-cell interactions (Figure 3b) [72]. Mannino et al. [26] developed a lymphoma model with a vascularized perfusable channel to recapitulate the interactions among cancer cells, immune cells, and ECs in a tumor microenvironment of large diffuse B-cell lymphoma (Figure 3c(i)). The perfusable channel lined with an endothelial monolayer was close to immune cells in the lymphoma, which was of high fidelity to the cancer environment.

In addition to the common single-tissue tumor models, tumor models may consist of multiple tissues. By extending the aforementioned lymphoma model, downstream effects could be investigated by constructing two adjacent hydrogel wells, one containing healthy cells and the other containing cancer cells, that were connected by an endothelialized channel [26] (Figure 3c(ii)). In another study, a connected tumor-liver model was created by Ozkan et al. [25] to evaluate the drug transport and toxicity to the liver tissue (Figure 3d) through a perfusable channel. The complex tumor model integrated with independent healthy tissues may enable the study of systemic effects of the tumor secretome, such as the waste syndrome that can occur in patients with advanced stage cancers.

Tumor models can also be utilized to study metastasis, the primary cause of death of cancer patients. Metastasis is highly dependent on the interactions between cancer cells and blood vessels. Engineered *in vitro* tumor models mimicking the intravasation and extravasation of tumor cells in the blood vessel network may aid the development of effective treatments to impair this essential process in metastasis [59]. Cui et al. [73] investigated the invasion of breast cancer cells into vascularized bone tissue using a triculture metastatic model (Figure 3e), which was developed using SLA. The co-culture of cancer cells, vascular cells, and bone cells allowed the study of cell-cell interactions during cancer progression. In another study on cancer cell intravasation, it was revealed that the tumor organoids could integrate into the endothelialized channel, thus forming mosaic vessels (Figure 3f) [28,74]. Mosaic vessel formation, vessel constriction, and vessel pull were observed as three types of tumor-vessel interactions. Meng et al. [75] investigated the key processes of the metastatic dissemination of cancer cells, including invasion, intravasation, and angiogenesis by a 3D printed vascularized metastatic model, where cellular behaviors were dynamically modulated by spatiotemporal control of signaling molecular gradients (Figure 3g).

Taken together, high-fidelity 3D tissue-engineered tumor platforms, which contain a physiologically realistic microenvironment by the incorporation of cell-cell interactions, leaky vasculature, and flow conditions, may enable future studies on tumor progression, invasion, and metastasis mechanisms, which could improve the translatability to preclinical investigations and lead to the identification of new therapeutic strategies to enhance clinical treatments[76-80].

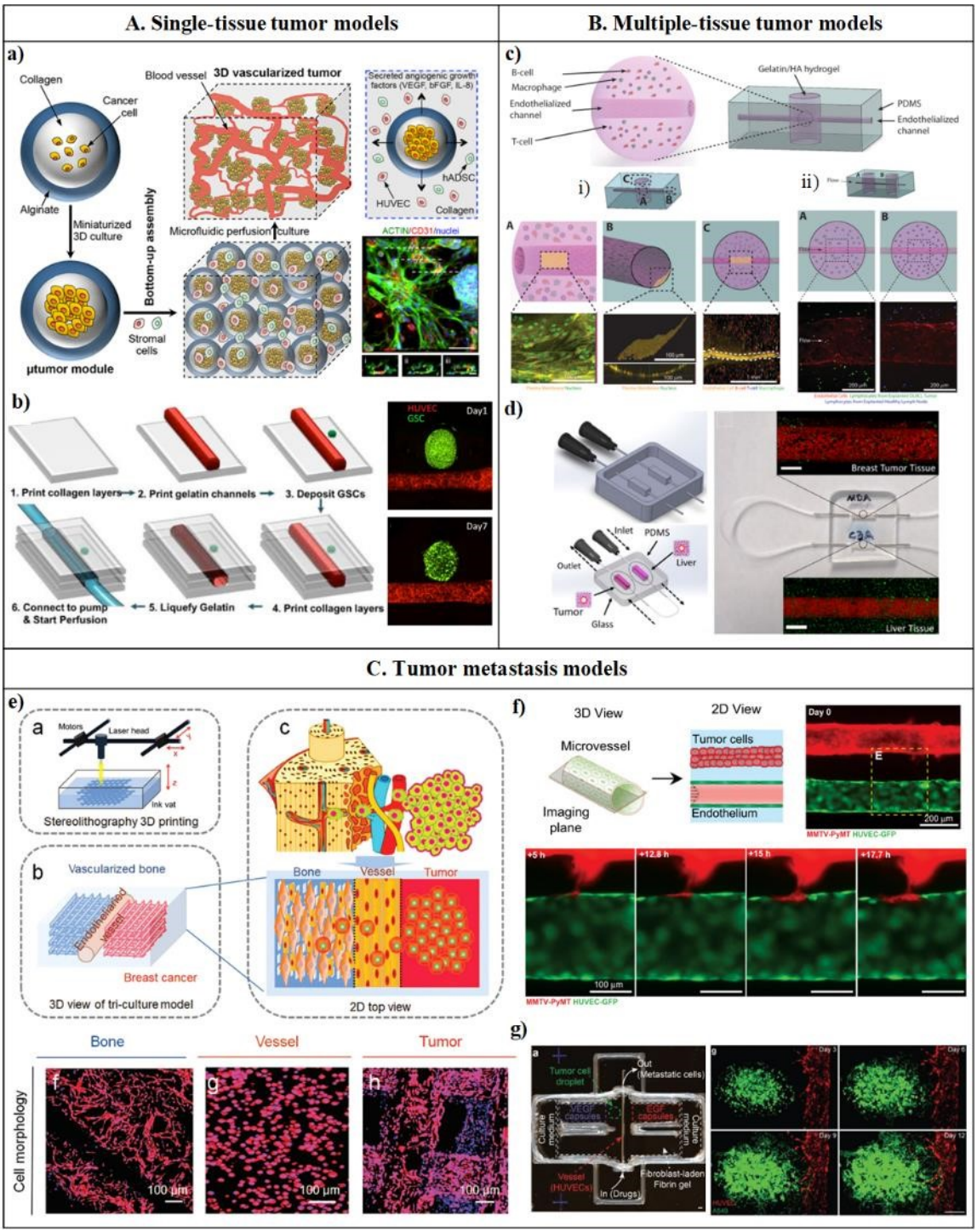

Figure 3. (A) Single-tissue tumor models. a) Bottom-up engineered vascularized tumor model [52]. b) Glioblastoma tumor model with perfusable channels [72]. (B) Multiple-tissue tumor models. c) Lymphoma models. (i) lymphoma model with a vascularized perfusable channel, (ii) connected tumor model of healthy and tumor tissues [26]. d) Connected tumor-liver model [25]. Confocal images show preconditioned tumorigenic and healthy vessels with GFP-tagged breast cancer cells and FITC-tagged anti-albumin immunostained healthy liver cells. (Scale bar: 500 μm). (C) Tumor metastasis models. e) Breast cancer metastasis to bone [73]. f) Intravasation of breast cancer cells into the vessel [28]. g) Tumor cell invasion and angiogenesis on a metastatic tumor model (scale bars: 500 μm) [75].

4.3. *In vitro* organ-level models

Human organs contain multiple functional tissues such as muscle, connective, and/or nervous tissues. Each tissue architecture usually requires a heterogeneous assemblage of significant numbers of cells and intercellular materials as well as dynamic remodeling of ECM. Generally, this architecture is far beyond a simple cellular arrangement layer by layer in a 3D space. While fully functional, full-size organs for clinical implantation are currently not available, tissue platforms with anatomically complex architectures and necessary mechanical properties and functionality are in high demand as *in vitro* organ-level models. Recent advances in the field of engineering 3D vascularized organ models, including heart, kidneys, liver, lungs, and brain, are described below.

4.3.1. **Heart**

Heart is responsible for continuously pumping blood throughout the body. As the central pivot of the circulatory system, it contains multiscale vessels ranging from arteries and veins of up to 25 mm in diameter to capillaries of several microns. A matured human heart contains approximately 9 billion cells, including cardiomyocytes (CMs), ECs, SMCs, fibroblasts, and others, with a relatively high capillary-to-cardiomyocyte ratio, indicating a high metabolic demand [81,82]. While the fabrication of a functional human heart is still a long way to go, heart components such as vascularized cardiac patches and heart-like structures have been investigated [83,84].

Cardiac patches can be used as tissue substitutes for damaged heart areas. A typical 3D biofabrication process to fabricate a cardiac patch include the selection of proper biomaterials, encapsulation of CMs and vascular cells (typically ECs), and fabrication of open lumens. Noor et al. [85] printed vascularized cardiac patches (as thick as 2 mm) with open lumens of 300 μm in diameter (Figure 4a(i)) by using direct extrusion printing. Two bioinks were utilized: one ink containing human induced pluripotent stem cells (iPSCs)-derived CMs and decellularized omentum hydrogels processed from humans or pigs and the other EC-based sacrificial ink. However, the resulting vascular network was limited due to insufficient functionality of the endothelial layers or formation of microvessels. Lee et al. [86] fabricated a vascularized cardiac construct with rat CMs, rat cardiac fibroblasts (CFs), and HUVECs encapsulated and a perfusable lumen (3 mm in diameter) at the center by embedded extrusion printing their customized cellular ink in a Carbopol support bath (Figure 4b), and verified the endothelium barrier function and synchronous beating of cardiac muscle cells in the printed construct. Long-term *in vitro* viability and functionality experiments were also conducted for up to 15 days to demonstrate its feasibility. However, the resulting 3D culture environment was under static conditions instead of being perfused, and the printed cardiac tissue model needed to be sectioned into 3 mm slices and cultured statically with medium changed every day. In terms of perfusable studies for engineered cardiac patches, Skylar-Scott et al. [38] utilized sacrificial ink-assisted embedded printing to fabricate perfusable diagonal arterial vascular networks in a cardiac tissue matrix containing human iPSC-derived embryoid bodies, organoids, or multicellular spheroids, followed by seeding HUVECs onto the inner wall (Figure 4c). In this study, the engineered tissue was perfused in oxygenated media by connecting to an external pump, and synchronous beating was demonstrated for up to 7 days.

Since the fabrication of full-size heart models with multiscale vascular networks is still a major challenge as of now, engineering heart-like structures with elementary anatomical features is of great interest. Both a subregion of the human heart and a neonatal-scale human heart that contained digitally designed branching networks were fabricated by embedded printing collagen in a gelatin

support bath (Figure 4d) [87]. This heart model included atrial and ventricular chambers, trabeculae, and pulmonary and aortic valves and was to be further cellularized with microscale vessels. Noor et al. [85] printed a small-scale human heart model using a human/pig omentum-based cellular ink (Figure 4a(ii)) as a milestone effort toward scale-up organ printing. Spatial organization of rat CMs and ECs was achieved by embedded printing using the two cellular inks, respectively, and hollow chambers were demonstrated alive one day post-printing; however, long-term construct survivability was not discussed, and the complexity of heart-related dense microvessel structures need to be established.

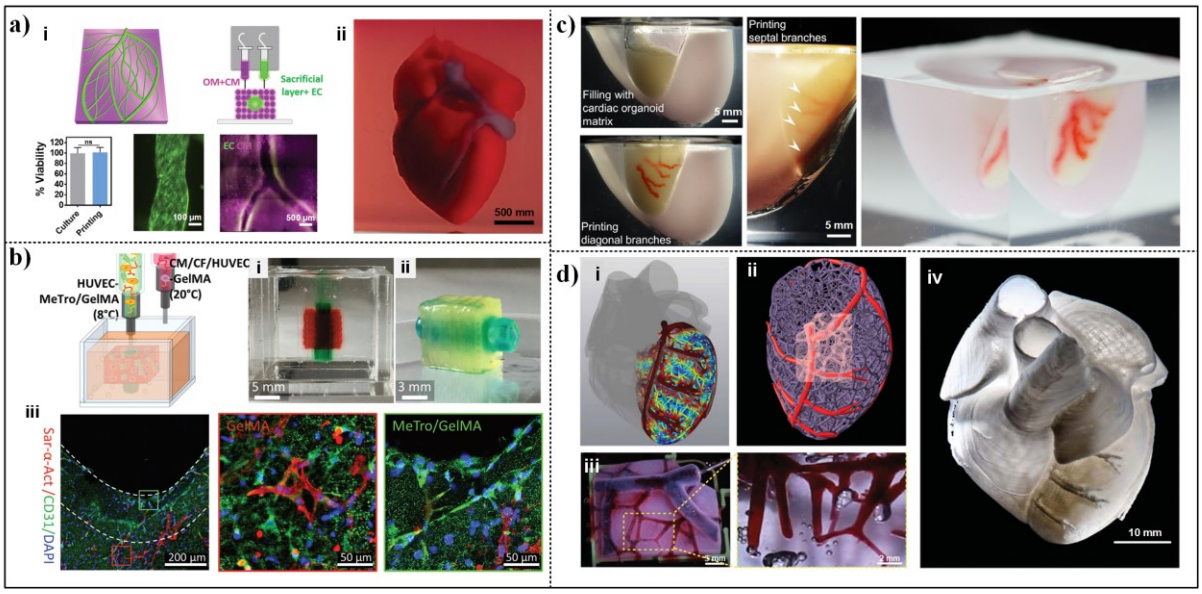

Figure 4. (a) Vascularized cardiac patch and perfusable heart-like structure [85]. (b) Vascularized cardiac constructs by (i,ii) embedded printing in a support bath and (iii) cross-sectional immunostaining results [86]. (c) Perfusable cardiac tissue with diagonal branches printed in cardiac organoid matrix [38]. (d) Perfusable vascularized human heart model generated from (i) a MRI-derived 3D human heart model (grey) with computationally derived multiscale vascular network (red to blue), (ii) a subregion (pink) printed for (iii) perfusion demonstration, and (iv) neonatal-scale human heart model as printed by FRESH using collagen [87].

4.3.2. **Kidney**

Kidney plays a major role in maintaining fluid homeostasis through continuously filtering the blood. A kidney is composed of over one million nephrons, and each nephron is the basic unit in the kidney that responsible for the material exchange and energy transmission, including the glomerulus filtering blood to form primary urine and renal tubules reabsorbing nutrients until final urine is formed passing by the collecting duct. The fast filtration highly relies on the efficient capillary exchange in the filtration unit. Therefore, a complex vascular network is an essential prerequisite for an engineered renal tissue to fulfill the requirements of cellular interactions. For glomerular and tubular tissue compartment fabrication, it can be achieved by seeding renal epithelial cells onto perfusable channels as EC seeding for creating vascularized tissues [88,89]. In this regard, epithelium-endothelium crosstalk can be an interesting topic after the construction of two adjacent channels (Figure 5a) using a microfluidic method. The feasibility was demonstrated to incorporate tubules and vascular networks to create a 3D vascularized proximal tubule model by Lin et al. [35] and enable studies on interactions between adjacent channels (Figure 5b). In Lin et al.'s model, active reabsorption via the tubular-vascular exchange that occurs in a native kidney

tissue was observed, and the epithelium-endothelium crosstalk was studied by inducing hyperglycemic conditions and EC dysfunction, which indicated potential in exploring other diseases associated with cellular interactions such as diabetes. Similarly, with the help of sacrificial-assisted coaxial printing, Singh et al. [90] created two adjacent hollow tubes, which were composed of renal tubular epithelial and endothelial cells, respectively, to mimic the renal proximal tubular physiological microenvironment (Figure 5c).

Despite the creation of macroscale perfusable channels with a diameter of several hundred microns to mimic the functional unit, microscale capillaries are also important for the survival of thick renal tissues, which have shown greater promise for ultimate transplantation applications. The recent introduction of kidney organoids, which exhibit enhanced angiogenesis by cellular self-assembly and maturation under perfusion (Figure 5d), may promote the microscale vascularization of renal tissue models [53]. The self-assembly principle of organoids can be a supplement to current engineering approaches [2] as it is still difficult to directly print microscale vasculature. Nevertheless, due to the significant structural complexity of kidneys, only simplified designs mimicking the microcirculation system in kidneys have been demonstrated to date.

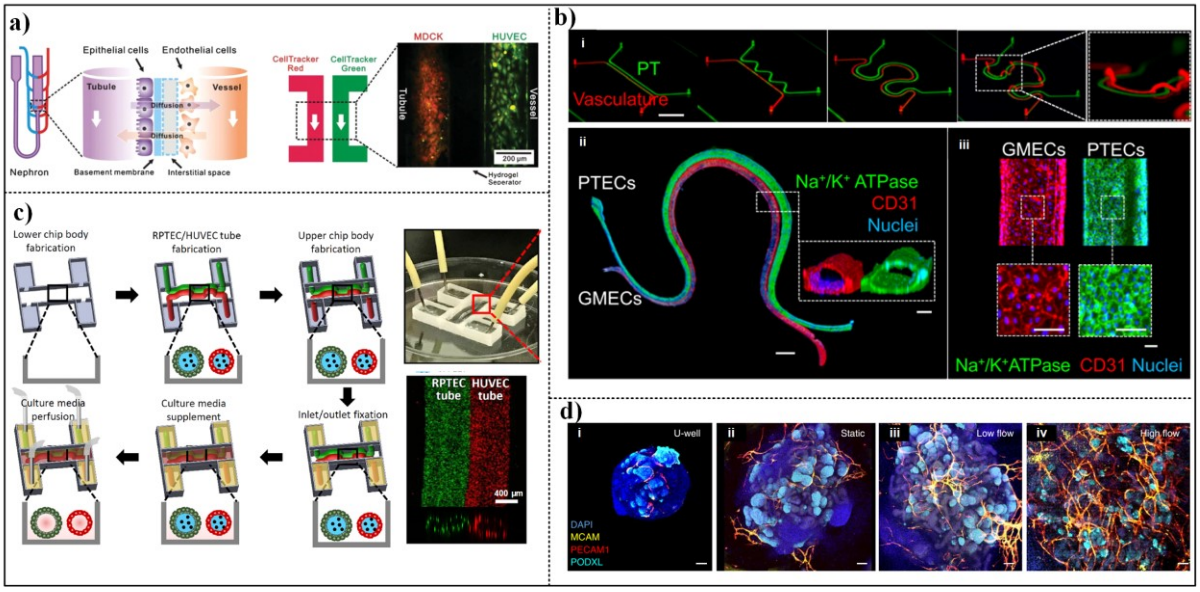

Figure 5. (a) Vascularized nephron model with two adjacent perfusable channels lined with epithelial cells and ECs, respectively [88]. (b) Vascularized proximal tubule models for study on renal reabsorption [35]. (i) Design of models (Scale bar: 10 mm). (ii) Immunofluorescence staining of the 3D tissue model (Scale bar: 1 mm). (Inset) Cross-sectional images of the two open lumens (scale bar: 100 μm). (iii) High-magnification images of the two lumens (scale bars: 100 μm). (c) Perfusable proximal tubular analogue fabricated by coaxial sacrificial printing [90]. (d) Confocal 3D rendering images of vascular markers in kidney organoids cultured under (i) static well, (ii) static engineered ECM, (iii) low flow, and (iv) high flow conditions, showing enhanced vascularization under a high flow condition (scale bars: 100 μm) [53].

4.3.3. **Liver**

The liver is the largest solid organ in the human body. It is responsible for various essential functions such as filtering the blood and detoxifying chemicals [82,91]. It is a complex and highly vascularized organ, largely composed of anatomic units called hepatic lobules. The hepatic lobule is a hexagonal structure that consists of a central vein located at the center, hepatocytes arranged into radiating cords from the central vein, and a portal triad of vessels at each of the six corners. The blood in the central veins and hepatic artery flows through the capillaries called sinusoids,

which serve as locations for the exchange of nutrients, oxygen, and xenobiotics with the surrounding hepatocytes. This vascular system plays a crucial role in liver function. Current treatments for severe liver disease including acute liver failure and end-stage liver disease are limited to liver transplantation, for which the shortage of donor organs remains a major problem [92].

Various efforts have been devoted to developing liver models with the hepatic lobule unit. Ma et al. [93] used the DLP-based printing technology to pattern multiple cell types into a hexagonal biomimetic architecture, where human induced pluripotent stem cells derived hepatic progenitor cells (hiPSC-HPCs) were encapsulated with the supporting cells including HUVECs and hADSCs to form a physiologically relevant cell diversity and liver microenvironment (Figure 6a). The supporting cells were responsible for the vascularization of the 3D liver tissue model, and both phenotypic and functional enhancements were demonstrated in this triculture system. However, the formation of vascular channels paved with an EC monolayer still needs further demonstration. Kang et al. [94] bioprinted a vascularized hepatic lobule structure with a central perfusable endothelialized lumen (150 μm) surrounded by hepatocytes with the help of a pre-set extruder (Figure 6b). The printed construct showed increased albumin and urea secretion due to the well-organized ECs and hepatocytes as well as the simultaneous interconnection of ECs. Larger perfusable channels were also fabricated using casting over a 3D printed template [95]. A four-arm-branched perfusable channel up to 1.3 mm in diameter was created within a liver hepatocellular carcinoma (HepG2) cell-laden matrix of 1 cm thick, mimicking a stiff and vascularized microenvironment of liver tumors (Figure 6c). Due to the perfusion culturing environment, the cells encapsulated within the thick tissue showed viability as a function of the distance from the perfusable channel, which can be utilized to study tumor necrotic regions. However, the endothelial barrier effect was not considered due to the absence of endothelization of the perfusable channel.

The angiogenesis concept has also been adopted for liver model development by the formation of capillary-like networks inside. Lee et al. [56] developed a co-culture system including hepatocytes, HUVECs, and HLFs within a 3D lattice scaffold using a multihead extrusion printing system (Figure 6d). Results showed that angiogenesis could benefit the construction of a 3D microenvironment, thereby increasing the survivability and functionality of hepatocytes. Mori et al. [96] fabricated a tube-shaped 3D liver-like tissue with an engineered macrochannel at the center by casting a collagen gel over a needle and further formed self-organized capillary-like structures by the lined ECs. Results showed that angiogenesis was promoted under the perfusion condition, and the flow through the main channel to the sinusoid-like structures was achievable.

The aforementioned liver models have the potential for the study of pharmacokinetics, pharmacodynamics, and metabolism of hepatocytes due to the existence of vascularized structures for the delivery of test substances into the tissue. In comparison to the 2D culturing environment, the continuous perfusion environment of the bioreactor can simulate the physiologically relevant cell shear stress and nutrient/drug supply for pharmacokinetic and pharmacodynamic study and high throughput drug screening. Microfluidics-based liver-on-a-chip devices have been developed for drug screening and toxicological effects on the liver, using matrix materials ranging from a rigid acellular polymer like PDMS [97] to cell-laden hydrogels [56,95] as a more realistic ECM environment. However, such biochip models usually have a thickness of only tens of microns, limited cell diversity and the lack of dense vasculature as significant shortcomings in recapitulating the complex native ECM environment.

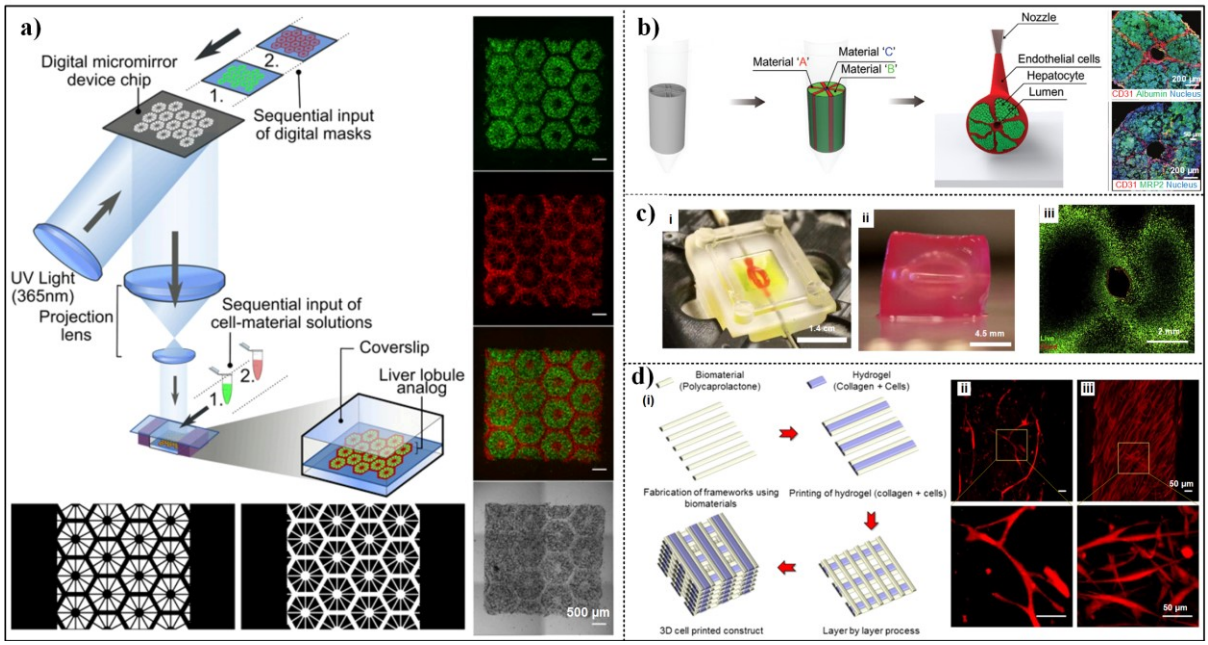

Figure 6. (a) Hexagonal hepatic construct fabricated by DLP with sequentially patterned hiPSC-HPCs (green) and supporting cells (red) [93]. (b) Biomimetic vascularized hepatic lobule structure fabricated by a pre-set extruder in a single pass [94]. (c) A branched perfusable channel (i) fabricated within a 3D HepG2 cell-laden matrix, (ii) after 24 h of direct perfusion, and (iii) live/dead staining results on Day 15 (cross-section) [95]. (d) 3D printed liver tissue scaffold with cell co-culture-enabled vascularization [56]. (i) Layer-by-layer assembly of the scaffold and capillary network formation in the printed collagen hydrogel on (ii) Day 10 and (iii) Day 14.

4.3.4. **Lung**

The lung is the primary organ of the respiratory system that is responsible for gas exchange. End-stage lung disease, for which lung transplantation is the only available treatment [98,99], is the third leading cause of death in the world. As an *ex vivo* approach, a de-epithelialized lung with preserved vascular endothelium was reported to serve as a patient-specific physiologic scaffold for vascularized lung engineering [98]. Even though it can be a solution to injured lung repair and transplantation, engineering *in vitro* lung models that replicate the extraordinary complexity and cellular diversity [98] remains a promising but unmet goal. It is also worth noting that, different from other static organs, the presence of continuous periodic breathing movement in the human lung is another bioengineering challenge for maintaining the construct integrity [100].

The blood-air or alveolar-capillary barrier in the human lung, the region where gas exchange occurs, is inseparable from the critical roles of intact vascular networks. Elaborate designs of lung-on-a-chip models have been reported in the past few years that successfully reconstituted the periodic breathing activity of the living lung and microstructure as well as the dynamic microenvironment of the alveolar-capillary unit [101-103]. Huh et al. [103] fabricated a breathing lung-on-a-chip by coating ECs and epitheliums on each side of a porous membrane to simulate the blood-air interface while applying alternant stretching/relaxation to simulate the breathing movement (Figure 7a). This organ-on-a-chip approach holds potential for drug screening and disease modeling due to the advantages of simplified architecture, compact design, and easy maintenance. Jain et al. [104] also reported a microfluidic lung alveolus-on-a-chip that contained two adjacent channels lined by epithelium and endothelium respectively to construct the interface under the perfusion of whole blood. Using this model, *in vitro* pulmonary thrombosis can be

induced by stimulating the platelet-endothelial interactions, which allows the further analysis of thrombotic responses to potential new therapies. Compared to animal models, one of the advantages of such *in vitro* models is that a specific factor can be decoupled from the complex *in vivo* environment to clarify its independent contribution. More recently, as a response to the global coronavirus disease pandemic in 2019 (known as COVID-19), microfluidic alveolus chips have been reported to model the organ-level lung infection and immune responses induced by severe acute respiratory syndrome coronavirus 2 (SARS-CoV-2) [105,106]. Despite the progress made with lung-on-a-chip models, a functional full-size lung with a hierarchical 3D structure and diverse cellular composition is still an elusive goal for ultimately clinical transplant applications.

Flow networks in human organs are physically and chemically entangled to provide a rich extracellular environment and enhance the transport of substances. To this end, Grigoryan et al. [45] developed a helix-shaped 3D vascular network wrapping around a serpentine-shaped airflow channel and verified the oxygen transport of infused red blood cells (Figure 7b). Furthermore, they also provided a vascularized alveolar model by introducing additional structural features of the native distal lung (Figure 7c). However, only macroscale vessel-like structures were engineered without generating micro vasculatures through angiogenesis. Regardless of some limitations, this model well mimicked the cyclic alveolar inflation and corresponding vessel compression, which can work as a delicate platform for intervascular transport and nutrient delivery studies.

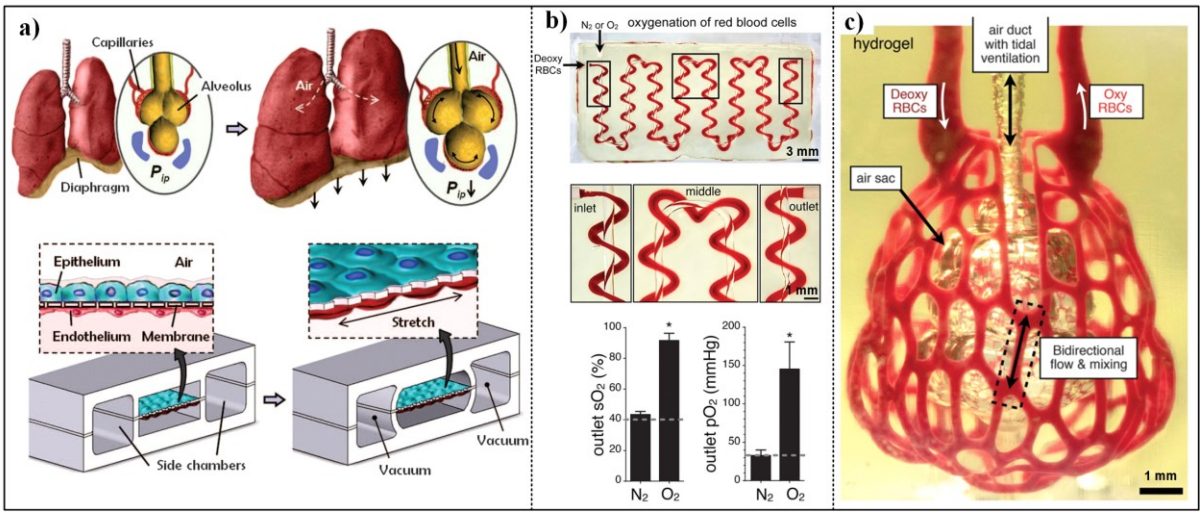

Figure 7. (a) Breathing lung-on-a-chip [103]. (b) Oxygenation of red blood cells within an entangled flow network embedded in a hydrogel, showing increased oxygen partial pressure (PO_2) and oxygen saturation (SO_2) at the outlet due to the gas diffusion, and (c) distal lung subunit with tidal air and blood flows [45].

4.3.5. **Brain**

Human brain only accounts for 2% of the body weight but consumes up to 20% of the body's energy, which is higher than any other organ. In brains, neurons and glial cells, estimated to number of 100 billion, represent 75–90% of the total volume [19]. Due to the high cell/ECM ratio and demanding metabolic requirements, dense vascular networks are critical for efficient oxygen and nutrition transport. Blood vessels in the brain are lined with a tight endothelial barrier, called the blood-brain barrier (BBB), that has a higher selective restriction on the exchange of chemical and biological substances than the capillary network of other organs. The BBB dysfunction is believed to be relevant to several neurodegenerative diseases such as Alzheimer's and Parkinson's

disease [107,108]. However, the high selectivity of the BBB restricts the delivery of pharmaceuticals and therapeutic antibodies to the central nervous system (CNS), which remains the main challenge for therapeutic development [109]. Towards this end, *in vitro* BBB models have been extensively studied, aiming at understanding the delivery mechanisms and developing new CNS-targeting therapeutics [109-113]. The general idea is to coat ECs and astrocytes/pericytes on the two sides of a porous membrane, respectively, to simulate the blood-brain interface. Similar to other microfluidic devices, they are limited in recapitulating the native physiological environment and overall functions due to the lack of complex 3D structure, vasculature, or diverse cellular composition. To improve the complexity of the BBB microenvironment and recapitulate the brain vascular morphogenesis with tight EC junctions, 3D tri-culture microfluidic models have been developed by culturing ECs, primary brain pericytes, and astrocytes within 3D fibrin gels; two adjacent perfusable medium channels, which can also be endothelialized by EC seeding, are located on the two sides of the gel for permeability investigation cross the central vascularized matrix [114-116].

In regard to vascularization, models made by the brain organoids engineering approach incorporated with microvasculature systems have emerged [117,118]. In such brain models, the endothelium can be induced and formed under environmental stimuli and further support the formation of blood vessels. In comparison to microfluidic chips, vascularized brain organoids can offer a physiological environment that is more relevant to the native tissue niche. Since the significant complexity of the brain and the challenge in forming large-scale perfusable vessels based on cellular self-assembly, the construction of scale-up brain tissues with multiscale vasculatures as well as heterogeneous architectures continues to require engineering and biological innovations.

5. Impact of pre-vascularization of engineered tissues on implantation and anastomosis *in vivo*

For applications related to implantation and anastomosis *in vivo*, pre-vascularization of engineered tissue grafts is indispensable since cellular activities are largely dependent on the availability of sufficient vasculature and blood perfusion. Given the slow native angiogenesis process, necrosis may happen before the formation of efficient capillary networks after the implantation of engineered tissue grafts. Fortunately, the *in vitro* vascularization of tissue constructs prior to implantation *in vivo* benefits the tissue survival through anastomosis with the host vasculature [119]. Recently, several studies have encapsulated vascular and support cells to achieve vascularized tissues *in vitro* and evaluated the efficacy and translational value of the vascularized tissues in animal models. Takebe et al. [120] introduced the generation of an iPSCs-derived vascularized liver bud by the organoid technology and showed hepatic maturation after implantation. Zhang et al. [121] employed a biodegradable elastomer to fabricate a built-in vascular scaffold (called AngioChip) by the microfluidics method, which contains microholes and nanopores on the walls for enhanced permeability and intercellular crosstalk. Since the stable perfusable vasculature helps the immediate establishment of blood perfusion, direct surgical anastomosis was demonstrated after a vascularized tissue was implanted to the femoral vessels of rat hind limbs [121]. More recently, a scaffold-free DLP method was investigated to construct a GelMA-based liver model (Figure 8a) with encapsulated HUVECs and mesenchymal cells for vasculature self-assembly [46]. After 2 weeks of subcutaneous implantation in mice, dense endothelial networks with red blood cells were observed, indicating a successful anastomosis between the engineered vasculature and the host *in situ*.

Various disease-specific implantation applications have been conducted to verify the *in vivo*

therapeutic effectiveness of vascularized tissue grafts [122-125]. In particular, some studies of ischemia, myocardial infarction, hypothyroidism, liver injury, and diabetes are described below. For ischemia, Mirabella et al. [126] reported the induced spontaneous collateral circulation in ischemia and myocardial infarction mouse models after implanting a 3D printed vascular patch graft containing EC-lined lumens (Figure 8b). They also found that the endothelialized microchannels arranged in parallel with a diameter of 400 μm presented a better anastomosis performance than those in a grid shape. For myocardial infarction, Redd et al. [127] demonstrated that engineered perfusable microvascular constructs showed a higher cardiomyocyte and vascular density after being implanted on infarcted rat hearts for 5 days, indicating the enhancement of pre-patterned vasculature on the vascular remodeling and coronary perfusion (Figure 8c). In a vascularized liver tissue implantation study using a rodent model of chronic liver injury, Grigoryan et al. [45] demonstrated that the microchannel networks integrated with the host blood and hepatocytes, resulting in an enhanced albumin promoter activity in the tissue graft (Figure 8d). In another hypothyroidism mouse model [128], the bioprinted vascularized thyroid gland construct normalized the blood thyroxine level and body temperature after grafting under the kidney capsule. Furthermore, other studies engineered vascularized islet organs and achieved normoglycemia after they were implanted in diabetic mice [55,129,130], which paved the path towards islet implantation and functionalization. A microvascular mesh was fabricated through the anchored self-assembly by vascular endothelial cells, and it could promote formation of functional blood vessels and anastomoses after transplantation (Figure 8e).

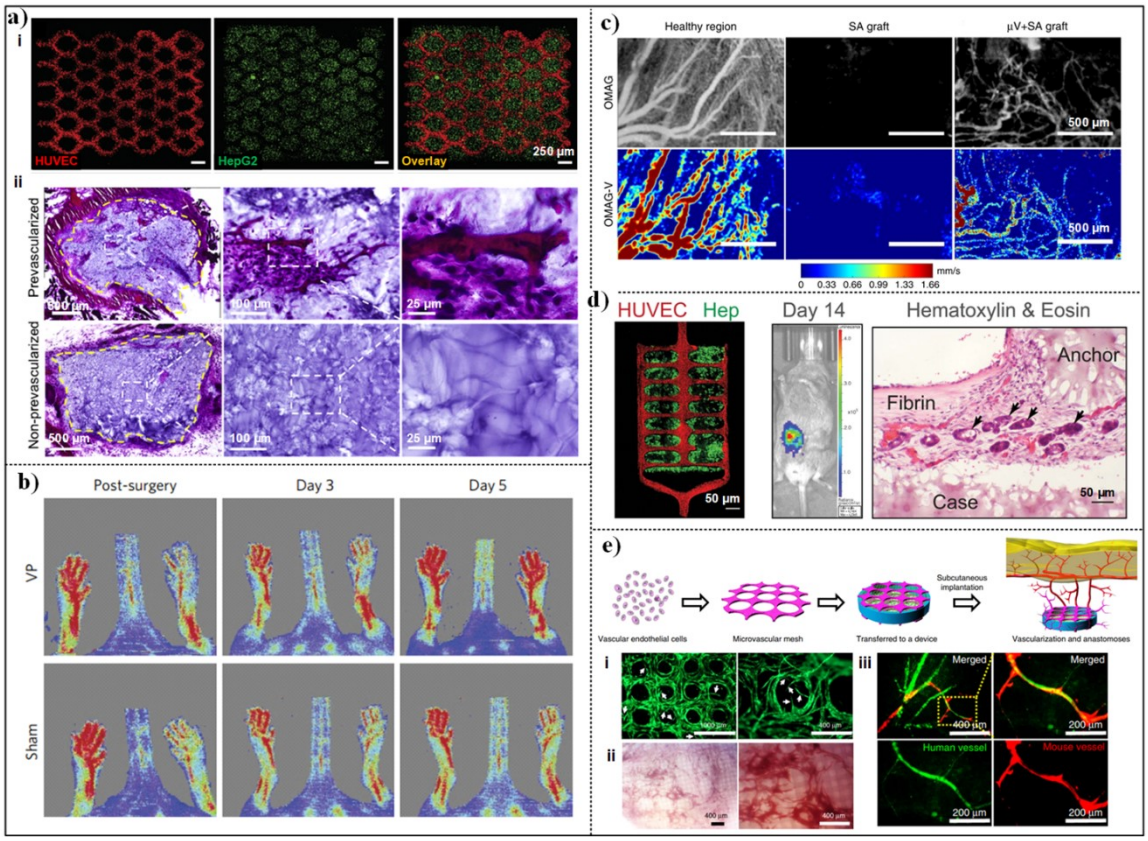

Figure 8. (a) In vitro vascularized tissue constructs (i) with patterned ECs for lumen-like structures formation and (ii) anastomosis after 2-week subcutaneous implantation [46]. (b) Laser Doppler images of hind limb ischaemia in a mouse model after implanted with a vascularized patch (VP), showing restored blood perfusion in comparison with no treatment (sham) [126]. (c) Implanted vascular constructs in infarcted rat heart model showing better integration with host myocardium [127]. (d) Hepatocyte aggregates carried by in vitro vascularized tissue construct show albumin promoter activity after implantation in mice with chronic liver injury [45]. (e) Subcutaneous islet implantation of microvascular meshes. (i) angiogenic sprouts (white arrows) in fibrin matrix after 2 weeks culture in vitro, (ii) vascularization after 2 weeks of subcutaneous implantation in SCID-Beige mice, and (iii) anastomoses between human and mouse vessels [129].

6. Summary and future perspectives

The vascular system is critical for the survival of engineered tissues and organs since it enables oxygen and nutrient transfer as well as metabolic waste clearance. In some organs, the vasculature also plays an important role in achieving organ-specific functions. For instance, for human kidneys and liver, a vessel network is indispensable for the fast and massive fluid exchange to achieve efficient filtration and metabolism. For human lungs and brain, the blood-air and blood-brain barriers are essential and functional units that control the exchange of substances. The engineering of (thick) vascularized tissues that recapitulate organ-specific structures, properties, and functions has attracted increasing interest due to the great potential in tissue engineering and regenerative medicine [131]. By creating a physiologically relevant environment, studies of basic biology, pathology, drug discovery/screening, and those linked to potential clinical applications can be enabled by using such *in vitro* models. To date, various engineering and cellular self-assembly methods have been developed to fabricate vascularized tissues. However, the focus of the design considerations varies in different application scenarios. For instance, not all engineered biomimetic models are intended for *in vivo* transplantation, so it is reasonable that the design requirements

should be classified into different levels. To this end, the emphasized roles and design requirements of vascularization in different application scenarios are summarized in Table 3. Table 4 summarizes the realizations of vascularized tissues based on the fabrication technologies, matrix materials, cell sources, construct thickness, and vessel size.

While great progress has been made, there are still hurdles to be overcome prior to clinical applications and commercialization.

1) Biofabrication technologies and biomaterials. Even though perfusable channels can be constructed within tissues, an intricate multiscale vascular network including large vessels and microvasculature networks to produce the physiologically relevant complexity remains a significant challenge. Thanks to bioprinting and other engineering advances [132-134] as enabling tools, the focus of this field has been advancing towards clinical applications. Furthermore, hybrid fabrication technologies such as hybrid printing technologies [18,135] that are able to effectively engineer a wide diameter range of vessels are expected to significantly facilitate the maturation of the organized vascular system. Besides the development of biofabrication technologies, cytocompatible, biodegradable biomaterials with desirable mechanical properties and tissue-specific stiffness are also greatly needed. Regulating the effects of matrix component networking with tunable cross-linking dynamics on cell mechanosensing and vascular morphogenesis is an interesting research direction for the innovative design of hydrogels.
2) Tissue complexity. The vascular system in the human body is a complex interconnected network that transports critical nutrients and oxygen throughout the body while minimizing energy cost. The branching geometry and structural hierarchy of the vascular tree should also be considered in order to engineer the intricate vascular network. Mathematical models have been established for the design of mother and daughter vessels [8]. Critical parameters such as the diameter, length, and bifurcation angle need to be taken into consideration when engineering vascularized tissue models. In addition to vessel geometry, full-scale organ engineering with biomimetic physiological features and functionalities is still facing significant obstacles due to the increasing size and complexity of organs and tissues. In addition, when scaling up a tissue in terms of size, the fabrication efficiency can be a further problem during real-time construction. While it is widely agreed that the establishment of intact, multiscale, and perfusable vascular networks is the prerequisite for tissue survival and function, questions on the minimally required biomimicry still remain when engineering a whole organ. While it is desirable to introduce as much structural complexity and cellular diversity and population as possible, breakthroughs in organ regeneration and morphosis mechanisms may help to better design a meta-phase of a final tissue construct.
3) Tissue-specific characteristics and cell sources. Ideally, the vascular bed can not only act as a conduit well but also exhibit advanced semi-permeable barrier functions that underscore inflammation and swelling. Due to the diversity of selective permeability of endothelial barriers in different organs, tissue-specific vasculature should be further introduced to create more specific and sophisticated models. To this end, EC resources should be selected carefully or differentiated from stem cells. However, as for the former, current cell sources for endothelialization are HUVECs, HMVECs, and iPSC-ECs due to well-established protocols, regardless of the organ types. As for the latter, the definitive protocol for differentiation and roles of inductive cues needs further research.

4) Organoid technology. More recently, organoid technology has shown great promise for vascularization based on the cellular self-organization mechanism [136]. It is worth noting that blood vessel organoids have been investigated to successfully replicate morphological, functional, and molecular features of human microvasculature [137]. Moreover, the organoid technology should be considered as a supplement to the currently available engineering strategies instead of a replacement or conflict [138]. As such, it is valuable if the organoid technology can be integrated with the engineering strategies to better direct cells in differentiation, self-organization, and functional specialization. Fortunately, a meaningful starting point has been occurring in this regard [139].
5) Vascularized organs as a system. To date, most of the research is limited to modeling a single organ environment without considering organ-organ interactions [86]. Systemic correlations involving different organs as well as immune and nervous systems will require extensive additional investigation.
6) Vessel regression and remodeling. The regression of formed vessels remains a significant technical difficulty that hinders the establishment of stable tissue models as constructed. The construction of long-standing vascular networks and the evolution of capillaries to arterioles and arterioles to arteries are among the most exciting tissue models for the time to come. In this regard, a deep understanding of basic vascular biology such as the vessel remodeling and the effects of hemodynamics on vasculature formation, is of great importance.
7) Vessel remodeling associated with diseased tissues. The vascular system is part of the whole tissue, maintaining tissue functions via blood perfusion and interplay with tissue cells and environment. Diseased tissues are often associated with altered angiogenic environments, resulting in microvascular network remodeling. Many age-associated pathological scenarios, including cancer, diabetes, hypertension, and myocardial ischemia, are associated with changes in network patterns, endothelial dysfunction, and/or altered vasoreactivity. Understanding the differences and associated mechanisms between healthy and diseased tissues at the network, vessel, and cellular levels is valuable for the development of clinical treatments.

Table 3. Summary of emphasized roles and design requirements of vascularization in different application scenarios.

Application scenario	Goal	Main roles of vascular structures	Special design requirements
Generic vessel models	Recapitulation of the vessel structures and functionalities of real tissues	Maintain the vascular functionalities such as EC barrier function, mass exchange, interactions with the blood components (e.g., platelets, red blood cells, leukocytes, etc.)	Mimic the multilayered vascular structure in real vessels, reproduce particular geometries or abnormal vascular segments as needed, manipulate the blood flow status, and monitor relevant biological processes
Construction of *in vitro* tissues and organ-like biomimetic models	Tissue construct survival	Enable mass transport	Neutralize the diffusion limits, establish a well-distributed perfusable channel network throughout the whole tissue construct, and scale up the tissue construct with a considerable size
	Recapitulation of the organ structures and functionalities of real organs	Maintain the functionalities of vessel-involved organ units such as blood-air barrier, brain-blood barrier, renal tubule, glomerulus, and hepatic lobule	Mimic the organ structures to a certain degree, co-culture the vascular cells and organ-specific cells, enable the mass exchange, filtration, and permeability, and monitor relevant biological processes
	Recapitulation of the tumor structures and microenvironment (for tumor research only)	Maintain biological interactions with the tumor	Co-culture cancer cells, vascular cells, immune cells, and/or other resident cells, and reproduce relevant biological processes such as tumor angiogenesis, invasion, and metastasis
Vascularized tissue grafts for implantation	Instantaneous integration with the host vasculature via anastomosis after implantation to ensure the tissue graft survival after implantation	Restore / replenish the local blood flow	Establish *in vitro* vascularization prior to the implantation, and encapsulate living cells and/or therapeutic substances as needed

Table 4. Summary of realizations of vascularized tissues ("/" indicates different application scenarios).

Realization		Fabrication technology	Matrix material	Cell source	Construct dimensions	Vessel size (diameter)	Reference
Generic vessel models	Vascular biology	Molding	Collagen	HUVECs, HBVPCs, HUASMCs	1 mm	100 μm	61
		Bioreactor (top-down approach)	Mesentery	Rat mesentery tissues	20–40 μm	Self-assembled micro vessels	54
		Molding (by stainless steel springs)	Collagen	HUVECs, tumor cells (KG1a, leukemia cells)	10 × 5 × 5 mm	400 μm	27
	Hematological disease	Molding (3D printed pluronic as sacrificial material)	GelMA without cells	HDFs, HUVECs	-	~1 mm	32
		Microfluidics	Agarose–gelatin interpenetrating polymer-network hydrogel without cells	HUVECs / HDMVECs / HLMVECs	-	20 μm	62
		Sacrificial-based embedded coaxial printing (SMCs-ECs-F127 triple coaxial cell printing)	Vascular tissue-derived decellularized ECM (VdECM)	HUVECs, HCASMCs, HDFs	-	600 ± 17 μm ~1540 ± 28 μm	63
Tumor models	Tumor environment	Microfluidics (bottom-up using	Collagen	MCF-7 human mammary cancer	5 × 1 × 0.5 mm (length	Self-assembled micro vessels	52

		microtumor capsules)		cells, HUVECs, hADSCs	width × depth)		
		Sacrificial-based extrusion printing (sandwich method, gelatin as the sacrificial material)	Collagen I	HUVECs, GSCs	3 mm	-	72
		Extrusion printing (sandwich method)	Collagen I	HUVECs, glioblastoma multiforme spheroid	2-2.5 mm	300-500 μm	140
		Molding (using stainless steel wire)	Gelatin / HA gel with Tumor cells	ECs	Φ4 mm × 1 mm (cylinder)	200 μm	26
		Molding (by solid objects)	Collagen I with telomerase - immortalized microvascular endothelial (TIME) cells	Human breast cancer cells (MDA - MB - 231), healthy liver cells (THLE - 3), carcinoma liver cells (C3Asub28)	-	435 μm, 711 μm	25
	Metastasis	SLA	GelMA, PEGDA with cells	HUVECs, breast cancer cell line (MDA-MB-231, MCF-7)	8 × 8 × 3 mm	500 μm	73
		Molding (by metal rod)	Rat tail collagen I, tumor organoids	HUVEC-GFP	-	~150 μm	28,74

		Molding	Fibroblast-laden fibrin gel	HUVECs	-	~300-500 μm	75
Organ-level models	Heart	Extrusion printing (Cardiac patch) and embedded printing (FRESH, whole heart)	Cell laden omentum gel	iPSCs-CMs and iPSCs-ECs (Cardiac patch) / rat neonatal CMs, HUVECs and fibroblasts (whole heart)	~2 mm (cardiac patch) / 7 × 7 × 7 mm (thick cardiac tissue) / 20 mm (whole heart)	~300 μm (cardiac patch) / ~1 mm (whole heart)	85
		Embedded printing (FRESH)	GelMA	CMs, CFs, and HUVECs	7.2 × 7.2 × 16.5 mm	3 mm	86
		Embedded sacrificial printing (SWIFT)	iPSC–derived organoid	HUVECs	4 mm	400 μm - 1 mm	38
		Embedded printing (FRESH)	Collagen	HUVECs	-	~100 μm - 5 mm	87
	Kidney	Molding (3D printed F127 as the sacrificial material)	Gelbrin (gelatin + fibrin)	PTECs, GMECs	-	~410 μm	35
		Coaxial sacrificial printing	Kidney dECM, alginate	REC (shell), EC (core) (filament) / HUVECs, RPTECs (chip)	-	~500-700 μm	90
		Microfluidics	Gelbrin (Gelatin + Fibrin) ECM	Kidney organoids	3.6 mm	Multiscale vessels	53
	Liver	DLP	GelMA, GM-HA	hiPSC-HPCs, HUVECs, ADSCs	~200 μm	-	93
		Preset cartridge	Collagen,	ECs, HepG2/C3A	1 mm in	150 μm	94

		extrusion bioprinting	alginate		diameter		
		Molding (3D printed PVA as the sacrificial material)	Gelatin	HepG2	1 cm	1.3 mm	95
		Scaffold (extrusion printing, co-culture)	Collagen	HUVECs:HLFs (1:3)	10.2 × 10.2 × 0.3 mm	Self-assembled micro vessels	56
		Molding (using metal rod)	Collagen	HUVECs, MSCs, HepG2	Elliptic cylinder of 2 (major axis) × 0.7 (minor axis) × 7 (length) mm	Multiscale vessels with engineered large vascular channel of 300 μm and self-assembled micro vessels	96
	Lung	SLA	PEGDA / mixture of PEGDA and GelMA	HUVECs, RBCs, HLFs, HLECs	34 × 17 × 6 mm	0.35-0.8 mm	45
	Brain	Microfluidics	Fibrin	hiPSC-ECs, primary brain pericytes, astrocytes	150 μm (height) × 2200 μm (width)	Endothelialized fluidic channels of 150 μm (height) × 1340 μm (width) and self-assembled micro vessels	114
		Microfluidics	Fibrin	HBMECs, primary human pericytes, primary normal human astrocytes, HLFs	120-150 μm (height) × 800 μm (width)	Endothelialized fluidic channels of 150 μm (height) × 650 μm (width) and	115

						self-assembled micro vessels	
In vitro vascularized tissue implantation	Anastomosis	Scaffold	POMaC elastomer	HUVECs	1.58-2 mm	100 µm × 50-100 µm	121
		DLP	GelMA, GM-HA	HUVECs:10T1/2 s (50:1)	4×5×0.6 mm	5-50 µm	46
	Disease-specific implantation	Molding (3D printed carbohydrate glass as sacrificial material)	Fibrin	HUVECs	> 2 mm	200 – 400 µm	126
		Molding	Collagen	hESC-ECs	1mm	100 µm	127
		SLA	Fibrin / GelMA (with hepatic aggregates)	HUVECs, NHDFs	4 mm	~20 µm	45
		Bottom-up	Collagen	Thyroid spheroids (known to produce high levels of VEGF-A) and allantoic spheroids as a source of thyrocytes and ECs	-	Self-assembled micro vessels	128
		Anchored self-assembly	Fibrin	HUVECs:NHDFs (9:1)	~25 µm	Self-assembled micro vessels	129
		Bioreactor	Cell medium	Decellularized rat lung lobe and ECs	-	Self-assembled micro vessels	55
		Scaffold (bottom-up)	Collagen	HUVECs	-	Self-assembled micro vessels	130

Acknowledgments

This research was partially supported by the US National Science Foundation (1762941), the Florida Breast Cancer Foundation, and the US National Institutes of Health (HL162405, U54CA233396, U54CA233444, & U54CA233465). The U54 grants support the Florida-California Cancer Research, Education and Engagement (CaRE2) Health Equity Center. The content is solely the responsibility of the authors and does not necessarily represent the official views of the National Institutes of Health. The final peer-reviewed manuscript is subject to the National Institutes of Health Public Access Policy.

Conflicts of Interests

The authors have no conflicts to disclose.

Data Availability

Data sharing is not applicable to this article as no new data were created or analyzed in this study.

Author Contributions

Bing Ren: Conceptualization; Writing/Original Draft Preparation. **Zhihua Jiang:** Writing/Review & Editing. **Walter Lee Murfee:** Writing/Review & Editing. **Adam J. Katz:** Writing/Review & Editing. **Dietmar Siemann**: Writing/Review & Editing. **Yong Huang:** Conceptualization; Writing/Review & Editing.

References

[1] M. Lovett, K. Lee, A. Edwards, and D.L. Kaplan, Tissue Eng. Part B Rev. **15** (3), 353-370 (2009).
[2] Yong Huang and Steven R. Schmid, J. MANUF. SCI. E. **140** (9) (2018).
[3] P. Sasmal, P. Datta, Y. Wu, and I. T. Ozbolat, Microphysiol. Syst. **2** (2018).
[4] A. Hasan, A. Paul, N. E. Vrana, X. Zhao, A. Memic, Y. S. Hwang, M. R. Dokmeci, and A. Khademhosseini, Biomaterials **35** (26), 7308-7325 (2014).
[5] F. A. Auger, L. Gibot, and D. Lacroix, Annu. Rev. Biomed. Eng. **15**, 177-200 (2013).
[6] P. Carmeliet and R.K. Jain, Nature **407** (6801), 249-257 (2000).
[7] L. Moroni, J. A. Burdick, C. Highley, S. J. Lee, Y. Morimoto, S. Takeuchi, and J. J. Yoo, Nat. Rev. Mater. **3** (5), 21-37 (2018).
[8] C. Tomasina, T. Bodet, C. Mota, L. Moroni, and S. Camarero-Espinosa, Materials (Basel) **12** (17) (2019).
[9] Guang Yang, Bhushan Mahadik, Ji Young Choi, and John P. Fisher, Prog. Biomed. Eng **2** (1), 012002 (2020).
[10] R. Xie, W. Zheng, L. Guan, Y. Ai, and Q. Liang, Small, e1902838 (2019).
[11] J. Rouwkema, N. C. Rivron, and C. A. van Blitterswijk, Trends Biotechnol. **26** (8), 434-441 (2008).
[12] O. I. Butt, R. Carruth, V. K. Kutala, P. Kuppusamy, and N. I. Moldovan, Tissue Eng. **13** (8), 2053-2061 (2007).
[13] E. C. Novosel, C. Kleinhans, and P. J. Kluger, Adv. Drug. Deliv. Rev. **63** (4-5), 300-311 (2011).
[14] J. Rouwkema and A. Khademhosseini, Trends Biotechnol. **34** (9), 733-745 (2016).
[15] R. W. Barrs, J. Jia, S. E. Silver, M. Yost, and Y. Mei, Chem. Rev. **120** (19), 10887-10949 (2020).
[16] Yi Zhang, Piyush Kumar, Songwei Lv, Di Xiong, Hongbin Zhao, Zhiqiang Cai, and

Xiubo Zhao, Mater. Design **199**, 109398 (2021).
[17] Sharon Fleischer, Daniel Naveed Tavakol, and Gordana Vunjak-Novakovic, Adv. Funct. Mater. **30** (37), 1910811 (2020).
[18] A. K. Miri, A. Khalilpour, B. Cecen, S. Maharjan, S. R. Shin, and A. Khademhosseini, Biomaterials **198**, 204-216 (2019).
[19] P. Datta, B. Ayan, and I. T. Ozbolat, Acta Biomater. **51**, 1-20 (2017).
[20] J. Schöneberg, F. De Lorenzi, B. Theek, A. Blaeser, D. Rommel, A. J. C. Kuehne, F. Kiessling, and H. Fischer, Sci. Rep. **8** (1), 10430 (2018).
[21] R. Marcu, Y. J. Choi, J. Xue, C. L. Fortin, Y. Wang, R. J. Nagao, J. Xu, J. W. MacDonald, T. K. Bammler, C. E. Murry, K. Muczynski, K. R. Stevens, J. Himmelfarb, S. M. Schwartz, and Y. Zheng, iScience **4**, 20-35 (2018).
[22] H. K. Wilson, S. G. Canfield, E. V. Shusta, and S. P. Palecek, Stem Cells **32** (12), 3037-3045 (2014).
[23] Y. Koui, T. Kido, T. Ito, H. Oyama, S. W. Chen, Y. Katou, K. Shirahige, and A. Miyajima, Stem Cell Rep. **9** (2), 490-498 (2017).
[24] U. Utzinger, B. Baggett, J. A. Weiss, J. B. Hoying, and L. T. Edgar, Angiogenesis **18** (3), 219-232 (2015).
[25] A. Ozkan, N. Ghousifam, P. J. Hoopes, T. E. Yankeelov, and M. N. Rylander, Biotechnol. Bioeng. **116** (5), 1201-1219 (2019).
[26] R. G. Mannino, A. N. Santiago-Miranda, P. Pradhan, Y. Qiu, J. C. Mejias, S. S. Neelapu, K. Roy, and W. A. Lam, Lab Chip **17** (3), 407-414 (2017).
[27] C. Mandrycky, B. Hadland, and Y. Zheng, Sci. Adv. **6** (38), eabb3629 (2020).
[28] V. L. Silvestri, E. Henriet, R. M. Linville, A. D. Wong, P. C. Searson, and A. J. Ewald, Cancer Res. **80** (19), 4288-4301 (2020).
[29] A. P. Golden and J. Tien, Lab Chip **7** (6), 720-725 (2007).
[30] X. Y. Wang, Z. H. Jin, B. W. Gan, S. W. Lv, M. Xie, and W. H. Huang, Lab Chip **14** (15), 2709-2716 (2014).
[31] A. Tocchio, M. Tamplenizza, F. Martello, I. Gerges, E. Rossi, S. Argentiere, S. Rodighiero, W. Zhao, P. Milani, and C. Lenardi, Biomaterials **45**, 124-131 (2015).
[32] Y. S. Zhang, F. Davoudi, P. Walch, A. Manbachi, X. Luo, V. Dell'Erba, A. K. Miri, H. Albadawi, A. Arneri, X. Li, X. Wang, M. R. Dokmeci, A. Khademhosseini, and R. Oklu, Lab Chip **16** (21), 4097-4105 (2016).
[33] I. S. Kinstlinger, S. H. Saxton, G. A. Calderon, K. V. Ruiz, D. R. Yalacki, P. R. Deme, J. E. Rosenkrantz, J. D. Louis-Rosenberg, F. Johansson, K. D. Janson, D. W. Sazer, S. S. Panchavati, K. D. Bissig, K. R. Stevens, and J. S. Miller, Nat. Biomed. Eng. **4** (9), 916-932 (2020).
[34] Sushila Maharjan, Jacqueline Alva, Cassandra Cámara, Andrés G. Rubio, David Hernández, Clément Delavaux, Erandy Correa, Mariana D. Romo, Diana Bonilla, Mille Luis Santiago, Wanlu Li, Feng Cheng, Guoliang Ying, and Yu Shrike Zhang, Matter (2020).
[35] N. Y. C. Lin, K. A. Homan, S. S. Robinson, D. B. Kolesky, N. Duarte, A. Moisan, and J. A. Lewis, Proc. Natl. Acad. Sci. U.S.A. **116** (12), 5399-5404 (2019).
[36] Shengyang Chen, Wen See Tan, Muhammad Aidil Bin Juhari, Qian Shi, Xue Shirley Cheng, Wai Lee Chan, and Juha Song, Biomed. Eng. Lett. (2020).
[37] W. Wu, A. DeConinck, and J. A. Lewis, Adv. Mater. **23** (24), H178-H183 (2011).
[38] M.A. Skylar-Scott, S.G. Uzel, L.L. Nam, J.H. Ahrens, R.L. Truby, S. Damaraju, and J.A. Lewis, Sci. Adv. **5** (9), eaaw2459 (2019).
[39] K.H. Song, C.B. Highley, A. Rouff, and J.A. Burdick, Adv. Funct. Mater. **28** (31), 1801331 (2018).
[40] N. Brandenberg and M. P. Lutolf, Adv. Mater. **28** (34), 7450-7456 (2016).

[41] C. K. Arakawa, B. A. Badeau, Y. Zheng, and C. A. DeForest, Adv. Mater. **29** (37), 1703156 (2017).
[42] W. Lee, V. Lee, S. Polio, P. Keegan, J. H. Lee, K. Fischer, J. K. Park, and S. S. Yoo, Biotechnol. Bioeng. **105** (6), 1178-1186 (2010).
[43] V. K. Lee, D. Y. Kim, H. Ngo, Y. Lee, L. Seo, S. S. Yoo, P. A. Vincent, and G. Dai, Biomaterials **35** (28), 8092-8102 (2014).
[44] L. Zhao, V. K. Lee, S. S. Yoo, G. Dai, and X. Intes, Biomaterials **33** (21), 5325-5332 (2012).
[45] B. Grigoryan, S. J. Paulsen, D. C. Corbett, D. W. Sazer, C. L. Fortin, A. J. Zaita, P.T. Greenfield, N.J. Calafat, J.P. Gounley, A.H. Ta, and F Johansson, Science **364** (6439), 458-464 (2019).
[46] W. Zhu, X. Qu, J. Zhu, X. Ma, S. Patel, J. Liu, P. Wang, C. S. Lai, M. Gou, Y. Xu, K. Zhang, and S. Chen, Biomaterials **124**, 106-115 (2017).
[47] Y. Shin, J. S. Jeon, S. Han, G. S. Jung, S. Shin, S. H. Lee, R. Sudo, R. D. Kamm, and S. Chung, Lab Chip **11** (13), 2175-2181 (2011).
[48] M. D. Sarker, S. Naghieh, N. K. Sharma, and X. Chen, J. Pharm. Anal. **8** (5), 277-296 (2018).
[49] N. Koike, D. Fukumura, O. Gralla, P. Au, J.S. Schechner, and R.K. Jain, Nature **428** (6979), 138-139 (2004).
[50] J. S. Schechner, A. K. Nath, L. Zheng, M. S. Kluger, C. C. Hughes, M. R. Sierra-Honigmann, M. I. Lorber, G. Tellides, M. Kashgarian, A. L. Bothwell, and J. S. Pober, Proc. Natl. Acad. Sci. U.S.A. **97** (16), 9191-9196 (2000).
[51] Y. C. Chen, R. Z. Lin, H. Qi, Y. Yang, H. Bae, J. M. Melero-Martin, and A. Khademhosseini, Adv. Funct. Mater. **22** (10), 2027-2039 (2012).
[52] P. Agarwal, H. Wang, M. Sun, J. Xu, S. Zhao, Z. Liu, K. J. Gooch, Y. Zhao, X. Lu, and X. He, ACS Nano **11** (7), 6691-6702 (2017).
[53] K. A. Homan, N. Gupta, K. T. Kroll, D. B. Kolesky, M. Skylar-Scott, T. Miyoshi, D. Mau, M. T. Valerius, T. Ferrante, J. V. Bonventre, J. A. Lewis, and R. Morizane, Nat. Methods **16** (3), 255-262 (2019).
[54] J. M. Motherwell, M. Rozenblum, P. V. G. Katakam, and W. L. Murfee, Tissue Eng. Part C Methods **25** (8), 447-458 (2019).
[55] A. Citro, P. T. Moser, E. Dugnani, T. K. Rajab, X. Ren, D. Evangelista-Leite, J. M. Charest, A. Peloso, B. K. Podesser, F. Manenti, S. Pellegrini, L. Piemonti, and H. C. Ott, Biomaterials **199**, 40-51 (2019).
[56] J. W. Lee, Y. J. Choi, W. J. Yong, F. Pati, J. H. Shim, K. S. Kang, I. H. Kang, J. Park, and D. W. Cho, Biofabrication **8** (1), 015007 (2016).
[57] S. Kim, H. Lee, M. Chung, and N. L. Jeon, Lab Chip **13** (8), 1489-1500 (2013).
[58] R. Tiruvannamalai Annamalai, A. Y. Rioja, A. J. Putnam, and J. P. Stegemann, ACS Biomater. Sci. Eng. **2** (11), 1914-1925 (2016).
[59] M. I. Bogorad, J. DeStefano, A. D. Wong, and P. C. Searson, Microcirculation **24** (5) (2017).
[60] J. Motherwell and W. L. Murfee, Nat. Biomed. Eng. **2** (6), 349-350 (2018).
[61] Ying Zheng, Junmei Chen, Michael Craven, Nak Won Choi, Samuel Totorica, Anthony Diaz-Santana, Pouneh Kermani, Barbara Hempstead, Claudia Fischbach-Teschl, José A. López, and Abraham D. Stroock, Proc. Natl. Acad. Sci. U.S.A. **109** (24), 9342-9347 (2012).
[62] Y. Qiu, B. Ahn, Y. Sakurai, C.E. Hansen, R. Tran, P.N. Mimche, R.G. Mannino, J.C. Ciciliano, T.J. Lamb, C.H. Joiner, and S.F. Ofori-Acquah, Nat. Biomed. Eng. **2** (6), 453-463 (2018).
[63] Ge Gao, Wonbin Park, Byoung Soo Kim, Minjun Ahn, Suhun Chae, Won-Woo Cho,

Jisoo Kim, Jae Yeon Lee, Jinah Jang, and Dong-Woo Cho, Adv. Funct. Mater. **31** (10), 2008878 (2021).
[64] W. Zheng, B. Jiang, D. Wang, W. Zhang, Z. Wang, and X. Jiang, Lab Chip **12** (18), 3441-3450 (2012).
[65] Y. S. Zhang, M. Duchamp, R. Oklu, L. W. Ellisen, R. Langer, and A. Khademhosseini, ACS Biomater. Sci. Eng. **2** (10), 1710-1721 (2016).
[66] M. Dey, B. Ayan, M. Yurieva, D. Unutmaz, and I. T. Ozbolat, Adv. Biol., e2100090 (2021).
[67] A. Sobrino, D. T. Phan, R. Datta, X. Wang, S. J. Hachey, M. Romero-Lopez, E. Gratton, A. P. Lee, S. C. George, and C. C. Hughes, Sci. Rep. **6**, 31589 (2016).
[68] Y. Nashimoto, R. Okada, S. Hanada, Y. Arima, K. Nishiyama, T. Miura, and R. Yokokawa, Biomaterials **229**, 119547 (2020).
[69] V. Brancato, J. M. Oliveira, V. M. Correlo, R. L. Reis, and S. C. Kundu, Biomaterials **232**, 119744 (2020).
[70] Jing Nie, Qing Gao, Jianzhong Fu, and Yong He, Adv. Healthc. Mater. **9** (7), 1901773 (2020).
[71] R. Lugano, M. Ramachandran, and A. Dimberg, Cell Mol Life Sci **77** (9), 1745-1770 (2020).
[72] V. K. Lee, G. Dai, H. Zou, and S.-S Yoo, in *In 41st Annual Northeast, Biomedical Engineering Conference (Nebec)* (IEEE, Piscataway, NJ, 2015), pp. 1-2.
[73] H. Cui, T. Esworthy, X. Zhou, S. Y. Hann, R. I. Glazer, R. Li, and L. G. Zhang, Adv. Healthc. Mater. **9** (15), e1900924 (2020).
[74] A. D. Wong and P. C. Searson, Cancer Res. **77** (22), 6453-6461 (2017).
[75] F. Meng, C. M. Meyer, D. Joung, D. A. Vallera, M. C. McAlpine, and A. Panoskaltsis-Mortari, Adv. Mater. **31** (10), e1806899 (2019).
[76] J. L. Albritton and J. S. Miller, Dis. Model. Mech. **10** (1), 3-14 (2017).
[77] P. Datta, M. Dey, Z. Ataie, D. Unutmaz, and I. T. Ozbolat, NPJ Precis. Oncol. **4**, 18 (2020).
[78] J. Jang, Bioengineering (Basel) **4** (3) (2017).
[79] Liang Ma, Yuting Li, Yutong Wu, Abdellah Aazmi, Bin Zhang, Hongzhao Zhou, and Huayong Yang, Bio-Des. Manuf. **3** (3), 227-236 (2020).
[80] S. Mao, Y. Pang, T. Liu, Y. Shao, J. He, H. Yang, Y. Mao, and W. Sun, Biofabrication **12** (4), 042001 (2020).
[81] X. Sun, W. Altalhi, and S. S. Nunes, Adv. Drug. Deliv. Rev. **96**, 183-194 (2016).
[82] C. Mota, S. Camarero-Espinosa, M. B. Baker, P. Wieringa, and L. Moroni, Chem. Rev. **120** (19), 10547-10607 (2020).
[83] T. Agarwal, G. M. Fortunato, S. Y. Hann, B. Ayan, K. Y. Vajanthri, D. Presutti, H. Cui, A. H. P. Chan, M. Costantini, V. Onesto, C. Di Natale, N. F. Huang, P. Makvandi, M. Shabani, T. K. Maiti, L. G. Zhang, and C. De Maria, Mater. Sci. Eng. C **124**, 112057 (2021).
[84] K. Elkhoury, M. Morsink, L. Sanchez-Gonzalez, C. Kahn, A. Tamayol, and E. Arab-Tehrany, Bioact. Mater. **6** (11), 3904-3923 (2021).
[85] N. Noor, A. Shapira, R. Edri, I. Gal, L. Wertheim, and T. Dvir, Adv. Sci. **6** (11), 1900344 (2019).
[86] S. Lee, E. S. Sani, A. R. Spencer, Y. Guan, A. S. Weiss, and N. Annabi, Adv. Mater. **32** (45), e2003915 (2020).
[87] A. Lee, A. R. Hudson, D. J. Shiwarski, J. W. Tashman, T. J. Hinton, S. Yerneni, J. M. Bliley, P. G. Campbell, and A. W. Feinberg, Science **365** (6452), 482-487 (2019).
[88] X. Mu, W. Zheng, L. Xiao, W. Zhang, and X. Jiang, Lab Chip **13** (8), 1612-1618

(2013).
[89] K. A. Homan, D. B. Kolesky, M. A. Skylar-Scott, J. Herrmann, H. Obuobi, A. Moisan, and J. A. Lewis, Sci. Rep. **6** (1), 34845 (2016).
[90] N. K. Singh, W. Han, S. A. Nam, J. W. Kim, J. Y. Kim, Y. K. Kim, and D. W. Cho, Biomaterials **232**, 119734 (2020).
[91] L. Ma, Y. Wu, Y. Li, A. Aazmi, H. Zhou, B. Zhang, and H. Yang, Adv. Healthc. Mater., e2001517 (2020).
[92] G. M. Abouna, Transplant. Proc. **40** (1), 34-38 (2008).
[93] X. Ma, X. Qu, W. Zhu, Y.S. Li, S. Yuan, H. Zhang, J. Liu, P. Wang, C.S.E. Lai, F. Zanella, and G.S. Feng, Proc. Natl. Acad. Sci. U.S.A. **113** (8), 2206-2211 (2016).
[94] D. Kang, G. Hong, S. An, I. Jang, W. S. Yun, J. H. Shim, and S. Jin, Small **16** (13), e1905505 (2020).
[95] C. R. Pimentel, S. K. Ko, C. Caviglia, A. Wolff, J. Emneus, S. S. Keller, and M. Dufva, Acta Biomater. **65**, 174-184 (2018).
[96] N. Mori, Y. Akagi, Y. Imai, Y. Takayama, and Y. S. Kida, Sci. Rep. **10** (1), 5646 (2020).
[97] N. S. Bhise, V. Manoharan, S. Massa, A. Tamayol, M. Ghaderi, M. Miscuglio, Q. Lang, Y. Shrike Zhang, S. R. Shin, G. Calzone, N. Annabi, T. D. Shupe, C. E. Bishop, A. Atala, M. R. Dokmeci, and A. Khademhosseini, Biofabrication **8** (1), 014101 (2016).
[98] N.V. Dorrello, B.A. Guenthart, J.D. O'Neill, J. Kim, K. Cunningham, Y.W. Chen, M. Biscotti, T. Swayne, H.M. Wobma, S.X. Huang, and H.W. Snoeck, Sci. Adv. **3** (8), e1700521 (2017).
[99] A. Mammoto and T. Mammoto, Front. Bioeng. Biotechnol. **7**, 318 (2019).
[100] M. Mori, K. Furuhashi, J. A. Danielsson, Y. Hirata, M. Kakiuchi, C. S. Lin, M. Ohta, P. Riccio, Y. Takahashi, X. Xu, C. W. Emala, C. Lu, H. Nakauchi, and W. V. Cardoso, Nat. Med. **25** (11), 1691-1698 (2019).
[101] A. O. Stucki, J. D. Stucki, S. R. Hall, M. Felder, Y. Mermoud, R. A. Schmid, T. Geiser, and O. T. Guenat, Lab Chip **15** (5), 1302-1310 (2015).
[102] Jesus Shrestha, Maliheh Ghadiri, Melane Shanmugavel, Sajad Razavi Bazaz, Steven Vasilescu, Lin Ding, and Majid Ebrahimi Warkiani, Organs-on-a-Chip **1**, 100001 (2019).
[103] D. Huh, B.D. Matthews, A. Mammoto, M. Montoya-Zavala, H.Y. Hsin, and D.E. Ingber, Science **328** (5986), 1662-1668 (2010).
[104] A. Jain, R. Barrile, A. D. van der Meer, A. Mammoto, T. Mammoto, K. De Ceunynck, O. Aisiku, M. A. Otieno, C. S. Louden, G. A. Hamilton, R. Flaumenhaft, and D. E. Ingber, Clin. Pharmacol. Ther. **103** (2), 332-340 (2018).
[105] M. Zhang, P. Wang, R. Luo, Y. Wang, Z. Li, Y. Guo, Y. Yao, M. Li, T. Tao, W. Chen, J. Han, H. Liu, K. Cui, X. Zhang, Y. Zheng, and J. Qin, Adv. Sci., 2002928 (2020).
[106] Di Huang, Tingting Liu, Junlong Liao, Sushila Maharjan, Xin Xie, Montserrat Pérez, Ingrid Anaya, Shiwei Wang, Alan Tirado Mayer, Zhixin Kang, Weijia Kong, Valerio Luca Mainardi, Carlos Ezio Garciamendez-Mijares, Germán García Martínez, Matteo Moretti, Weijia Zhang, Zhongze Gu, Amir M. Ghaemmaghami, and Yu Shrike Zhang, Proc. Natl. Acad. Sci. U.S.A. **118** (19), e2016146118 (2021).
[107] C. Iadecola, Nat. Rev. Neurosci. **5** (5), 347-360 (2004).
[108] G. Boka, P. Anglade, D. Wallach, F. Javoy-Agid, Y. Agid, and E.C. Hirsch, Neurosci. Lett. **172** (1–2), 151-154 (1994).
[109] T. E. Park, N. Mustafaoglu, A. Herland, R. Hasselkus, R. Mannix, E. A. FitzGerald, R. Prantil-Baun, A. Watters, O. Henry, M. Benz, H. Sanchez, H. J. McCrea, L. C.

Goumnerova, H. W. Song, S. P. Palecek, E. Shusta, and D. E. Ingber, Nat. Commun. **10** (1), 2621 (2019).
[110] H. Cho, J. H. Seo, K. H. Wong, Y. Terasaki, J. Park, K. Bong, K. Arai, E. H. Lo, and D. Irimia, Sci. Rep. **5**, 15222 (2015).
[111] S. I. Ahn, Y. J. Sei, H. J. Park, J. Kim, Y. Ryu, J. J. Choi, H. J. Sung, T. J. MacDonald, A. I. Levey, and Y. Kim, Nat. Commun. **11** (1), 175 (2020).
[112] Y. Shin, S. H. Choi, E. Kim, E. Bylykbashi, J. A. Kim, S. Chung, D. Y. Kim, R. D. Kamm, and R. E. Tanzi, Adv. Sci. **6** (20), 1900962 (2019).
[113] Y.I. Wang, H.E. Abaci, and M.L. Shuler, Biotechnol. Bioeng. **114** (1), 184-194 (2017).
[114] S. W. L. Lee, M. Campisi, T. Osaki, L. Possenti, C. Mattu, G. Adriani, R. D. Kamm, and V. Chiono, Adv Healthc Mater **9** (7), e1901486 (2020).
[115] S. Lee, M. Chung, S. R. Lee, and N. L. Jeon, Biotechnol Bioeng **117** (3), 748-762 (2020).
[116] C. Hajal, G. S. Offeddu, Y. Shin, S. Zhang, O. Morozova, D. Hickman, C. G. Knutson, and R. D. Kamm, Nat Protoc **17** (1), 95-128 (2022).
[117] B. Cakir, Y. Xiang, Y. Tanaka, M. H. Kural, M. Parent, Y. J. Kang, K. Chapeton, B. Patterson, Y. Yuan, C. S. He, M. S. B. Raredon, J. Dengelegi, K. Y. Kim, P. Sun, M. Zhong, S. Lee, P. Patra, F. Hyder, L. E. Niklason, S. H. Lee, Y. S. Yoon, and I. H. Park, Nat. Methods **16** (11), 1169-1175 (2019).
[118] A. A. Mansour, J. T. Goncalves, C. W. Bloyd, H. Li, S. Fernandes, D. Quang, S. Johnston, S. L. Parylak, X. Jin, and F. H. Gage, Nat. Biotechnol. **36** (5), 432-441 (2018).
[119] Jan D. Baranski, Ritika R. Chaturvedi, Kelly R. Stevens, Jeroen Eyckmans, Brian Carvalho, Ricardo D. Solorzano, Michael T. Yang, Jordan S. Miller, Sangeeta N. Bhatia, and Christopher S. Chen, Proc. Natl. Acad. Sci. U.S.A. **110** (19), 7586-7591 (2013).
[120] T. Takebe, R. R. Zhang, H. Koike, M. Kimura, E. Yoshizawa, M. Enomura, N. Koike, K. Sekine, and H. Taniguchi, Nat. Protoc. **9** (2), 396-409 (2014).
[121] B. Zhang, M. Montgomery, M. D. Chamberlain, S. Ogawa, A. Korolj, A. Pahnke, L. A. Wells, S. Masse, J. Kim, L. Reis, A. Momen, S. S. Nunes, A. R. Wheeler, K. Nanthakumar, G. Keller, M. V. Sefton, and M. Radisic, Nat. Mater. **15** (6), 669-678 (2016).
[122] Z. Xing, C. Zhao, S. Wu, C. Zhang, H. Liu, and Y. Fan, Biomaterials **274**, 120872 (2021).
[123] P. Rukavina, F. Koch, M. Wehrle, K. Trondle, G. Bjorn Stark, P. Koltay, S. Zimmermann, R. Zengerle, F. Lampert, S. Strassburg, G. Finkenzeller, and F. Simunovic, Biotechnol. Bioeng. **117** (12), 3902-3911 (2020).
[124] T. Sasagawa, T. Shimizu, S. Sekiya, Y. Haraguchi, M. Yamato, Y. Sawa, and T. Okano, Biomaterials **31** (7), 1646-1654 (2010).
[125] M. A. Nazeer, I. C. Karaoglu, O. Ozer, C. Albayrak, and S. Kizilel, APL bioeng. **5** (2), 021503 (2021).
[126] T. Mirabella, J. W. MacArthur, D. Cheng, C. K. Ozaki, Y. J. Woo, M. Yang, and C. S. Chen, Nat. Biomed. Eng. **1** (2017).
[127] M. A. Redd, N. Zeinstra, W. Qin, W. Wei, A. Martinson, Y. Wang, R. K. Wang, C. E. Murry, and Y. Zheng, Nat. Commun. **10** (1), 584 (2019).
[128] E. A. Bulanova, E. V. Koudan, J. Degosserie, C. Heymans, F. D. Pereira, V. A. Parfenov, Y. Sun, Q. Wang, S. A. Akhmedova, I. K. Sviridova, N. S. Sergeeva, G. A. Frank, Y. D. Khesuani, C. E. Pierreux, and V. A. Mironov, Biofabrication **9** (3), 034105 (2017).

[129] W. Song, A. Chiu, L. H. Wang, R. E. Schwartz, B. Li, N. Bouklas, D. T. Bowers, D. An, S. H. Cheong, J. A. Flanders, Y. Pardo, Q. Liu, X. Wang, V. K. Lee, G. Dai, and M. Ma, Nat. Commun. **10** (1), 4602 (2019).
[130] A. E. Vlahos, S. M. Kinney, B. R. Kingston, S. Keshavjee, S. Y. Won, A. Martyts, W. C. W. Chan, and M. V. Sefton, Biomaterials **232**, 119710 (2020).
[131] J. Lee, D. Park, Y. Seo, J. J. Chung, Y. Jung, and S. H. Kim, Adv. Mater. **32** (51), e2002096 (2020).
[132] B. Ren, K. Song, A.R. Sanikommu, Y. Chai, M.A. Longmire, W. Chai, W.L. Murfee, and Y. Huang, Appl. Phys. Rev. **9** (1), 011408 (2022).
[133] G. Dai, A. W. Feinberg, and L. Q. Wan, Cell. Mol. Bioeng., 1-16 (2021).
[134] Q. Zhang, È. Bosch-Rué, R. A. Pérez, and G. A. Truskey, APL bioeng. **5** (2), 021507 (2021).
[135] Y. Jin, W. Chai, and Y. Huang, ACS Appl. Mater. Interfaces **10** (34), 28361-28371 (2018).
[136] E. Garreta, R. D. Kamm, S. M. Chuva de Sousa Lopes, M. A. Lancaster, R. Weiss, X. Trepat, I. Hyun, and N. Montserrat, Nat. Mater. (2020).
[137] R. A. Wimmer, A. Leopoldi, M. Aichinger, N. Wick, B. Hantusch, M. Novatchkova, J. Taubenschmid, M. Hammerle, C. Esk, J. A. Bagley, D. Lindenhofer, G. Chen, M. Boehm, C. A. Agu, F. Yang, B. Fu, J. Zuber, J. A. Knoblich, D. Kerjaschki, and J. M. Penninger, Nature **565** (7740), 505-510 (2019).
[138] F. Zheng, Y. Xiao, H. Liu, Y. Fan, and M. Dao, Adv. Biol., e2000024 (2021).
[139] J. A. Brassard, M. Nikolaev, T. Hubscher, M. Hofer, and M. P. Lutolf, Nat. Mater. **20** (1), 22-29 (2021).
[140] M. S. Ozturk, V. K. Lee, H. Zou, R. H. Friedel, X. Intes, and G. Dai, Sci. Adv. **6** (10), eaay7513 (2020).